

1 **Precipitation changes in the Mediterranean basin during**  
2 **the Holocene from terrestrial and marine pollen records: A**  
3 **model/data comparison**

4  
5 **Odile Peyron<sup>1</sup>, Nathalie Combourieu-Nebout<sup>2</sup>, David Brayshaw<sup>3</sup>, Simon Goring<sup>4</sup>,**  
6 **Valérie Andrieu-Ponel<sup>5</sup>, Stéphanie Desprat<sup>6,7</sup>, Will Fletcher<sup>8</sup>, Belinda Gambin<sup>9</sup>,**  
7 **Chryssanthi Ioakim<sup>10</sup>, Sébastien Joannin<sup>1</sup>, Ulrich Kotthoff<sup>11</sup>, Katerina Kouli<sup>12</sup>,**  
8 **Vincent Montade<sup>1</sup>, Jörg Pross<sup>13</sup>, Laura Sadori<sup>14</sup>, Michel Magny<sup>15</sup>**

9 [1] Institut des Sciences de l'Evolution (ISEM), Université de Montpellier, France

10 [2] UMR 7194 MNHN, Institut de Paléontologie Humaine 1, Paris, France

11 [3] University of Reading, Department of Meteorology, United Kingdom

12 [4] Department of Geography, Univ. of Wisconsin-Madison, Wisconsin, USA

13 [5] Institut Méditerranéen de Biodiversité et d'Ecologie marine et continentale (IMBE), Aix Marseille  
14 Université, Aix-en-Provence, France

15 [6] EPHE, PSL Research University, Laboratoire Paléoclimatologie et Paléoenvironnements Marins,  
16 Pessac, France

17 [7] Univ. Bordeaux, EPOC UMR 5805, Pessac, France

18 [8] Geography, School of Environment, Education and Development, University of Manchester, United  
19 Kingdom

20 [9] Institute of Earth Systems, University of Malta, Malta

21 [10] Institute of Geology and Mineral Exploration, Athens, Greece

22 [11] Center for Natural History and Institute of Geology, Hamburg University, Hamburg, Germany

23 [12] Department of Geology and Geoenvironment, National and Kapodistrian University of Athens, Greece

24 [13] Paleoenvironmental Dynamics Group, Institute of Earth Sciences, Heidelberg University, Germany

25 [14] Dipartimento di Biologia Ambientale, Università di Roma "La Sapienza", Roma, Italy

26 [15] UMR 6249 Chrono-Environnement, Université de Franche-Comté, Besançon, France

27 Correspondence to: O. Peyron ([odile.peyron@univ-montp2.fr](mailto:odile.peyron@univ-montp2.fr))

28 Abstract

29 Climate evolution of the Mediterranean region during the Holocene exhibits strong spatial and  
30 temporal variability which is notoriously difficult for models to reproduce. We propose here a  
31 new paleo-observations synthesis and its comparison – at regional (few ~100km) level – with  
32 a regional climate model to examine (i) opposing northern and southern precipitation regimes,  
33 and (ii) an east-to-west precipitation dipole during the Holocene across the Mediterranean  
34 basin. Using precipitation estimates inferred from marine and terrestrial pollen archives, we  
35 focus on the early to mid-Holocene (8000 to 6000 cal yrs BP) and the late Holocene (4000 to  
36 2000 yrs BP), to test these hypotheses on a Mediterranean-wide scale. Special attention was  
37 given to the reconstruction of season-specific climate information, notably summer and winter  
38 precipitation. The reconstructed climatic trends corroborate the north-south partition of  
39 precipitation regimes during the Holocene. During the early Holocene, relatively wet conditions  
40 occurred in the south-central and eastern Mediterranean region, while drier conditions prevailed  
41 from 45°N northwards. These patterns then reverse during the late Holocene. With regard to  
42 the existence of a west-east precipitation dipole during the Holocene, our results show that the  
43 strength of this dipole is strongly linked to the seasonal parameter reconstructed; early Holocene  
44 summers show a clear east-west division, with summer precipitation having been highest in  
45 Greece and the eastern Mediterranean and lowest over the Italy and the western Mediterranean.  
46 Summer precipitation in the east remained above modern values, even during the late Holocene  
47 interval. In contrast, winter precipitation signals are less spatially coherent during the early  
48 Holocene but low precipitation is evidenced during the late Holocene. A general drying trend  
49 occurred from the early to the late Holocene, particularly in the central and eastern  
50 Mediterranean.

51 For the same time intervals, pollen-inferred precipitation estimates were compared with model  
52 outputs, based on a regional-scale downscaling (HadRM3) of a set of global climate-model  
53 simulations (HadAM3). The high-resolution detail achieved through the downscaling is  
54 intended to enable a better comparison between ‘site-based’ paleo-reconstructions and gridded  
55 model data in the complex terrain of the Mediterranean; the model outputs and pollen-inferred  
56 precipitation estimates show some overall correspondence, though modeled changes are small  
57 and at the absolute margins of statistical significance. There are suggestions that the eastern  
58 Mediterranean experienced wetter than present summer conditions during the early and late  
59 Holocene; the drying trend in winter from the early to the late Holocene also appears to be  
60 simulated. The use of this high-resolution regional climate model highlights how the inherently

61 patchy” nature of climate signals and palaeo-records in the Mediterranean basin may lead to  
62 local signals much stronger than the large-scale pattern would suggest. Nevertheless, the east  
63 to west division in summer precipitation seems more marked in the pollen reconstruction than  
64 in the model outputs. The footprint of the anomalies (like today or dry winters, wet summers)  
65 has some similarities to modern analogue atmospheric circulation patterns associated with a  
66 strong westerly circulation in winter (positive AO/NAO) and a weak westerly circulation in  
67 summer associated with anti-cyclonic blocking; although there also remain important  
68 differences between the palaeo-simulations and these analogues. The regional climate model,  
69 consistent with other global models, does not suggest an extension of the African summer  
70 monsoon into the Mediterranean; so the extent to which summer monsoonal precipitation may  
71 have existed in the southern and eastern Mediterranean during the mid-Holocene remains an  
72 outstanding question.

73  
74

## 75 **1 Introduction**

76 The Mediterranean region is particularly sensitive to climate change due to its position within  
77 the confluence of arid North African (i.e. subtropically influenced) and temperate/humid  
78 European (i.e. mid-latitude) climates (Lionello, 2012). Palaeoclimatic proxies, including  
79 stable isotopes, lipid biomarkers, palynological data and lake-levels, have shown that the  
80 Mediterranean region experienced climatic conditions that varied spatially and temporally  
81 throughout the Holocene (e.g. Bar-Matthews and Ayalon, 2011; Luterbacher et al., 2012;  
82 Lionello, 2012; Triantaphyllou et al., 2014, 2016; Mauri et al., 2015; De Santis and Caldara  
83 2015; Sadori et al., 2016a; Cheddadi and Khater, 2016) and well before (eg. Sadori et al.,  
84 2016b). Clear spatial climate patterns have been identified from east to west and from north to  
85 south within the basin (e.g. Zanchetta et al., 2007; Magny et al., 2009b, 2011, 2013; Zhornyak  
86 et al., 2011; Sadori et al., 2013; Fletcher et al., 2013). Lake-level reconstructions from Italy thus  
87 suggest contrasting patterns of palaeohydrological changes for the central Mediterranean during  
88 the Holocene (Magny et al., 2012, 2013). Specifically, lake level maxima occurred south of  
89 approximately 40°N in the early to mid-Holocene, while lakes north of 40°N recorded minima.  
90 This pattern was reversed at around 4500 cal yrs BP (Magny et al., 2013). Quantitative pollen-  
91 based precipitation reconstructions from sites in northern Italy indicate humid winters and dry  
92 summers during the early to mid-Holocene, whereas southern Italy was characterised by humid  
93 winters and summers; the N-S pattern reverses in the late Holocene, with drier conditions at  
94 southern sites and wet conditions at northern sites (Peyron et al., 2011, 2013). These findings  
95 support a north–south partition for the central Mediterranean with regards to precipitation, and  
96 also confirm that precipitation seasonality is a key parameter in the evolution of Mediterranean  
97 climates. The pattern of shifting N-S precipitation regimes has also been identified for the  
98 Aegean Sea (Peyron et al., 2013). Taken together, the evidence from pollen data and from other  
99 proxies covering the Mediterranean region suggest a climate response that can be linked to a  
100 combination of orbital, ice-sheet and solar forcings (Magny et al., 2013).

101 An east-west pattern of climatic change during the Holocene is also suggested in the  
102 Mediterranean region (e.g. Combourieu Nebout et al., 1998; Geraga et al., 2010; Colmenero-  
103 Hildago et al., 2002; Kotthoff et al., 2008; Dormoy et al., 2009; Finné et al., 2011; Roberts et  
104 al., 2011, 2012; Luterbacher et al., 2012; Guiot and Kaniewski, 2015). An east-west division  
105 during the Holocene is observed from marine and terrestrial pollen records (Dormoy et al.,  
106 2009; Guiot and Kaniewski, 2015), lake-level reconstructions (Magny et al., 2013) and  
107 speleothem isotopes (Roberts et al. 2011).

108 This study aims to reconstruct and evaluate N-S and E-W precipitations patterns for the  
109 Mediterranean basin, over two key periods in the Holocene, the early Holocene 8000-6000 cal  
110 yrs BP, corresponding to the “Holocene climate optimum” and the late Holocene 4000-2000  
111 cal yrs BP corresponding to a trend towards drier conditions. Precipitation reconstructions are  
112 particularly important for the Mediterranean region given that precipitation rather than  
113 temperature represents the dominant controlling factor on the Mediterranean environmental  
114 system during the early to mid-Holocene (Renssen et al., 2012). Moreover, the reconstruction  
115 of precipitation parameters seems robust for the Mediterranean area (Combourieu-Nebout et  
116 al., 2009; Mauri et al., 2015; Peyron et al., 2011, 2013; Magny et al., 2013).

117 Precipitation is estimated for five pollen records from Greece, Italy and Malta, and for eight  
118 marine pollen records along a longitudinal gradient from the Alboran Sea to the Aegean Sea.  
119 Because precipitation seasonality is a key parameter of change during the Holocene in the  
120 Mediterranean (Rohling et al., 2002; Peyron et al., 2011; Mauri et al., 2015), the quantitative  
121 climate estimates focus on reconstructing changes in summer and winter precipitation.

122 Paleoclimate proxy data are essential benchmarks for model intercomparison and validation  
123 (e.g. Morrill et al., 2012; Heiri et al., 2014). This holds particularly true considering that  
124 previous model-data intercomparisons have revealed substantial difficulties for GCMs in  
125 simulating key aspects of mid-Holocene climate (Hargreaves et al., 2013) for Europe and  
126 notably for southern Europe (Davis and Brewer, 2009; Mauri et al., 2014). We also aim to  
127 identify and quantify the spatio-temporal climate patterns in the Mediterranean basin for the  
128 two key intervals of the Holocene (8000–6000 and 4000–2000 cal yrs BP) based on regional-  
129 scale climate model simulations (Brayshaw et al., 2011a). Finally, we compare our pollen-  
130 inferred climate patterns with regional-scale climate model simulations in order to critically  
131 assess the consistency of the climate reconstructions revealed by these two complimentary  
132 routes.

133 The first originality of our approach is that we estimate the magnitude of precipitation changes  
134 and reconstruct climatic trends across the Mediterranean using both terrestrial and marine high-  
135 resolution pollen records. The signal reconstructed is then more regional than in the studies  
136 based on terrestrial records alone. Moreover, this study aims to reconstruct precipitations  
137 patterns for the Mediterranean basin over two key periods in the Holocene while the existing  
138 large-scale quantitative paleoclimate reconstructions for the Holocene are often limited to the  
139 mid-Holocene - 6000 yrs BP- (Cheddadi et al., 1997; Bartlein et al., 2011; Mauri et al., 2014),  
140 except the climate reconstruction for Europe proposed by the study of Mauri et al. (2015).

141 The second originality of our approach is that we propose a data/model comparison based on  
142 (1) two time-slices and not only the mid-Holocene, a standard benchmark time period for this  
143 kind of data–model comparison; (2) a high resolution regional model (RCM) which provides a  
144 better representation of local/regional processes and helps to better simulate the localized,  
145 “patchy”, impacts of Holocene climate change, when compared to coarser global GCMs (e.g.  
146 Mauri et al., 2014); (3) changes in seasonality, particularly changes in summer atmospheric  
147 circulation which have not been widely investigated (Brayshaw et al., 2011).

148

## 149 **2 Sites, pollen records, and models**

150 The Mediterranean region is at the confluence of continental and tropical air masses.  
151 Specifically, the central and eastern Mediterranean is influenced by monsoonal systems, while  
152 the north-western Mediterranean is under stronger influence from mid-latitude climate regimes  
153 (Lionello et al., 2006). Mediterranean winter climates are strongly affected by storm systems  
154 originating over the Atlantic. In the western Mediterranean, precipitation is predominantly  
155 affected by the North Atlantic Oscillation (NAO), while several systems interact to control  
156 precipitation over the northern and eastern Mediterranean (Giorgi and Lionello, 2008).  
157 Mediterranean summer climates are dominated by descending high pressure systems that lead  
158 to dry/hot conditions, particularly over the southern Mediterranean where climate variability is  
159 strongly influenced by African and Asian monsoons (Alpert et al., 2006) with strong  
160 geopotential blocking anomalies over central Europe (Giorgi and Lionello, 2008; Trigo et al.,  
161 2006).

162 The palynological component of our study combines results from five terrestrial and eight  
163 marine pollen records to provide broad coverage of the Mediterranean basin (Fig. 1, Table 1).  
164 The terrestrial sequences comprise pollen records from lakes along a latitudinal gradient from  
165 northern Italy (Lakes Ledro and Accesa) to Sicily (Lake Pergusa), one pollen record from Malta  
166 (Burmarrad) and one pollen record from Greece (Tenaghi Philippon). The marine pollen  
167 sequences are situated along a longitudinal gradient across the Mediterranean Sea; from the  
168 Alboran Sea (ODP Site 976 and core MD95-2043), Siculo-Tunisian strait (core MD04-2797),  
169 Adriatic Sea (core MD90-917), and Aegean Sea (cores SL152, MNB-3, NS14, HCM2/22). For  
170 each record we used the chronologies as reported in the original publications (see Table 1 for  
171 references).

172 Climate reconstructions for summer and winter precipitation (Figs. 2 and 3) inferred from the  
173 terrestrial sequences and marine pollen records were performed for two key intervals of the  
174 Holocene: 8000–6000 cal yrs BP and 4000–2000 cal yrs BP; the climate values available during  
175 each period have been averaged. We use here the Modern Analogue Technique (MAT; Guiot,  
176 1990), a method which compares fossil pollen assemblages to modern pollen assemblages with  
177 known climate parameters. The MAT is calibrated using an expanded surface pollen dataset  
178 with more than 3600 surface pollen samples from various European ecosystems (Peyron et al.,  
179 2013). In this dataset, 2200 samples are from the Mediterranean region, and the results shows  
180 that the analogues selected here are limited to the Mediterranean basin. Since the MAT uses the  
181 distance structure of the data and essentially performs local fitting of the climate parameter (as  
182 the mean of  $n$ -closest sites), it may be less susceptible to increased noise in the data set, and  
183 less likely to report spurious values than others methods (for more details on the method, see  
184 Peyron et al., 2011). *Pinus* is overrepresented in marine pollen samples (Heusser and Balsam,  
185 1977; Naughton et al., 2007), and as such *Pinus* pollen was removed from the assemblages  
186 (both modern and fossil) for the calibration of marine records using MAT. The reliability of  
187 quantitative climate reconstructions from marine pollen records has been tested using marine  
188 core-top samples from the Mediterranean in Combourieu-Nebout et al. (2009), which shows an  
189 adequate consistency between the present day observed and MAT estimations for annual and  
190 summer precipitations values, however the MAT seems to overestimate the winter precipitation  
191 reconstructions in comparison with the observed values. More top-cores are needed to validate  
192 these results at the scale of the Mediterranean basin, particularly in the eastern part where only  
193 one marine top core was available (Combourieu-Nebout et al., 2009).

194 The climate model simulations used in the model-data comparison are taken from Brayshaw et  
195 al. (2010, 2011a, 2011b). The HadAM3 global atmospheric model (resolution 2.5° latitude x  
196 3.75° longitude, 19 vertical levels; Pope et al., 2000) is coupled to a slab ocean (HadSM3,  
197 Hewitt et al., 2001) and used to perform a series of time slice experiments. Each time-slice  
198 simulation corresponds to 20 model years after spin up (40 model years for pre-industrial). The  
199 time slices correspond to “present-day” (1960-1990), 2000 cal BP, 4000 cal BP, 6000 cal BP  
200 and 8000 cal BP conditions, and are forced with appropriate insolation (associated with changes  
201 in the Earth’s orbit), and atmospheric CO<sub>2</sub> and CH<sub>4</sub> concentrations. The heat fluxes in the ocean  
202 are held fixed using values taken from a pre-industrial control run (i.e., the ocean ‘circulation’  
203 is assumed to be invariant over the time-slices) and there is no sea-level change, but sea-surface  
204 temperatures are allowed to evolve freely. The coarse global output from the model for each

205 time slice is downscaled over the Mediterranean region using HadRM3 (i.e. a limited area  
206 version of the same atmospheric model; resolution  $0.44^\circ \times 0.44^\circ$ , with 19 vertical levels). Unlike  
207 the global model, HadRM3 is not coupled to an ocean model; instead, sea-surface temperatures  
208 are derived directly from the HadSM3 output.

209 Following Brayshaw et al. (2011a), time slice experiments are grouped into “mid Holocene”  
210 (8000 BP and 6000 cal yrs BP) and “late Holocene” (4000 BP and 2000 cal yrs BP) experiments  
211 because (1) these two periods are sufficiently distant in the past to be substantially different  
212 from the present but close enough that the model boundary conditions are well known; (2) these  
213 two periods are rich in high resolution and well-dated palaeoecological sequences, providing a  
214 good spatial coverage suitable for large-scale model-data comparison. The combination of the  
215 simulations into two experiments (Mid- and Late- Holocene) rather than assessing the two  
216 extreme timeslices (2000 and 8000 cal yrs BP) is intended to increase the signal-to-noise ratio  
217 by doubling the quantity of data in each experiment. This is necessary and possible as the  
218 change in forcing between adjacent time-slices is relatively small, making it difficult to detect  
219 differences between each individual simulations. To aid comparison with proxies, changes in  
220 climate are expressed as differences with respect to the present day (roughly 1960-1990) rather  
221 than the pre-industrial control run: therefore the climate anomalies shown thus include a  
222 component which is attributable to anthropogenic increases in greenhouse gases in the  
223 industrial period, as well as longer term ‘natural’ changes (e.g., orbital forcing). We suggest it  
224 may be better to use ‘present day’ to be in closer agreement with the pollen data (modern  
225 samples) which use the late 20th century long-term averages (1961-1990). However, there are  
226 some quite substantial differences between model runs under ‘present day’ and ‘preindustrial’  
227 forcings (Figure 4). Statistical significance is assessed with the Wilcoxon-Mann-Whitney  
228 significance test (Wilks, 1995).

229 The details of the climate model simulations are discussed at length in Brayshaw et al (2010,  
230 2011a, 2011b). These includes a detailed discussion of verification under present climate, the  
231 model’s physical/dynamical climate responses to Holocene period ‘forcings’, and comparison  
232 to other palaeoclimate modelling approaches (e.g., PMIP projects) and palaeo-climate  
233 syntheses. The GCM used (HadAM3 with a slab ocean) is comparable to the climate models in  
234 PMIP2, but a key advantages of the present dataset is: (a) the inclusion of multiple time-slices  
235 across the Holocene period; and (b) the additional high-resolution regional climate model  
236 downscaling enables the impact of local climatic effects within larger-scale patterns of change  
237 to be distinguished (e.g., the impact of complex topography or coastlines; Brayshaw et al

238 2011a), potentially allowing clearer comparisons between site-based proxy-data and model  
239 output.

240

### 241 **3 Results and Discussion**

242

#### 243 *A North-South precipitation pattern?*

244 Pollen evidence shows contrasting patterns of palaeohydrological changes in the central  
245 Mediterranean. The early- to mid-Holocene was characterized by precipitation maxima south  
246 of around 40°N while at the same time, northern Italy experienced precipitation minima; this  
247 pattern reverses after 4500 cal yrs BP (Magny et al., 2012b; Peyron et al., 2013). Other proxies  
248 suggest contrasting north-south hydrological patterns not only in central Mediterranean but also  
249 across the Mediterranean (Magny et al., 2013), suggesting a more regional climate signal. We  
250 focus here on two time periods (early to mid-Holocene and late Holocene), in order to test this  
251 hypothesis across the Mediterranean, and to compare the results with regional climate  
252 simulations for the same time periods.

#### 253 Early to mid-Holocene (8000 to 6000 cal yrs BP)

254 Climatic patterns reconstructed from both marine and terrestrial pollen records seem to  
255 corroborate the hypothesis of a north-south division in precipitation regimes during the  
256 Holocene (Fig 2a). Our results confirm that northern Italy was characterized by drier conditions  
257 (relative to modern) while the south-central Mediterranean experienced more annual, winter  
258 and summer precipitation during the early to mid-Holocene (Fig. 2a). Only Burmarrad (Malta)  
259 shows drier conditions in the early to mid-Holocene (Fig 2a), although summer precipitation  
260 reconstructions are marginally higher than modern at the site. Wetter summer conditions in the  
261 Aegean Sea suggest a regional, wetter, climate signal over the central and eastern  
262 Mediterranean. Winter precipitation in the Aegean Sea is less spatially coherent than summer  
263 signal, with dry conditions in the North Aegean Sea and or near-modern conditions in the  
264 Southern Aegean Sea (Figs. 2a and 3).

265 Non-pollen proxies, including marine and terrestrial biomarkers (terrestrial n-alkanes), indicate  
266 humid mid-Holocene conditions in the Aegean Sea (Triantaphyllou et al., 2014, 2016). Results  
267 within the Aegean support the pollen-based reconstructions, but non-pollen proxy data are still  
268 lacking at the basin scale in the Mediterranean, limiting our ability to undertake independent  
269 evaluation of precipitation reconstructions.

270 Very few large-scale climate reconstruction of precipitation exist for the whole Holocene (Guiot  
271 and Kaniewski, 2015; Tarroso et al., 2016) and, even at local scales, pollen-inferred  
272 reconstructions of seasonal precipitation are very rare (e.g. Peyron et al., 2011, 2013;  
273 Combourieu-Nebout et al., 2013; Nourelbait et al., 2016). Several « large-scale » studies focused  
274 on the 6000 cal years BP period (Cheddadi et al., 1997 ; Wu et al., 2007 ; Bartlein et al., 2011;  
275 Mauri et al., 2014). Wu et al. (2007) reconstruct regional seasonal and annual precipitation and  
276 suggest that precipitation did not differ significantly from modern conditions across the  
277 Mediterranean; however, scaling issues render it difficult to compare their results with the  
278 reconstructions presented here. Cheddadi et al. (1997) reconstruct wetter-than-modern conditions  
279 at 6000 yrs cal BP in southern Europe; however, their study uses only one record from Italy and  
280 measures the moisture availability index, which is not directly comparable to precipitation *sensu*  
281 *stricto*, since it integrates temperature and precipitation. At 6000 yrs cal BP, Bartlein et al. (2011)  
282 reconstruct Mediterranean precipitation at values between 100 and 500 mm higher than modern.  
283 Mauri et al. (2015), in an updated version of Davis et al. (2003), provide a quantitative climate  
284 reconstructions comparable to the seasonal precipitation reconstructions presented here.  
285 Compared to Davis et al. (2003), which focused on reconstruction of temperatures, Mauri et al.  
286 (2015) reconstructed seasonal precipitation for Europe and analyse their evolution throughout  
287 the Holocene. Mauri et al. (2015) results differ from the current study in using MAT with plant  
288 functional type scores and in producing gridded climate maps. Mauri et al. (2015) show wet  
289 summers in southern Europe (Greece and Italy) with a precipitation maximum between 8000 and  
290 6000 cal yrs BP, where precipitation was ~20 mm/month higher than modern. As in our  
291 reconstruction, precipitation changes in the winter were small and not significantly different from  
292 present-day conditions. Our reconstructions are in agreement with Mauri et al. (2015), with  
293 similar to present day summer conditions above 45°N during the early Holocene and wetter than  
294 today summer conditions over much of the south-central Mediterranean south of 45°N, while  
295 winter conditions appear to be similar to modern values. Mauri et al. (2015) results inferred from  
296 terrestrial pollen records and the climatic trends reconstructed here from marine and terrestrial  
297 pollen records seem to corroborate the hypothesis of a north-south division in precipitation  
298 regimes during the early to mid-Holocene in central Mediterranean. However, more high-  
299 resolution above 45°N are still needed to validate this hypothesis.

300 Late Holocene (4000 to 2000 cal yrs BP)

301 Late Holocene reconstructions of winter and summer precipitation indicate that the pattern  
302 established during the early Holocene was reversed by 4000 cal yrs BP, with similar to present

303 day or lower than present day precipitation in southern Italy, Malta and Siculo-Tunisian strait  
304 (Figs. 2b and 3). Annual precipitation reconstructions suggest drying relative to the early  
305 Holocene, with modern conditions in northern Italy, and modern conditions or drier than  
306 modern conditions in central and southern Italy during most of the late Holocene.  
307 Reconstructions for the Aegean Sea still indicate higher than modern summer and annual  
308 precipitation (Fig. 2b). Winter conditions reverse the early to mid-Holocene trend, with modern  
309 conditions in the northern Aegean Sea and wetter than modern conditions in the southern  
310 Aegean Sea (Fig. 3). Our reconstructions from all sites show a good fit with Mauri et al. (2015),  
311 except for the Alboran Sea where we reconstruct relatively high annual precipitations, whereas  
312 Mauri et al. (2015) reconstruct dry conditions, but here too, more sites are needed to confirm  
313 or refute this pattern in Spain. Our reconstruction of summer precipitation for the eastern  
314 Mediterranean is very similar to Mauri et al. (2015) where wet conditions are reported for  
315 Greece and the Aegean Sea.

316  
317 *An East-West precipitation pattern?*

318 A precipitation gradient, or an east-west division during the Holocene has been suggested for  
319 the Mediterranean from pollen data and lakes isotopes (e.g. Dormoy et al., 2009; Roberts et al.,  
320 2011; Guiot and Kaniewski, 2015). However, lake-levels and other hydrological proxies around  
321 the Mediterranean Basin do not clearly support this hypothesis and rather show contrasting  
322 hydrological patterns south and north of 40°N particularly during the Holocene climatic  
323 optimum (Magny et al., 2013).

324 Early to mid-Holocene (8000 to 6000 cal yrs BP)

325 The pollen-inferred annual precipitation indicates unambiguously wetter than today conditions  
326 south of 42°N in the western, central and eastern Mediterranean, except for Malta (Fig. 3). A  
327 prominent feature of the summer precipitation signal is an east-west dipole with increasing  
328 precipitation in the eastern Mediterranean (as for annual precipitation). In contrast, winter  
329 conditions show less spatial coherence, although the western basin, Sicily and the Siculo-  
330 Tunisian strait appear to have experienced higher precipitation than modern, while drier  
331 conditions exist in the east and in north Italy (Fig. 2a).

332 Our reconstruction shows a good match to Guiot and Kaniewski (2015) who have also discussed  
333 a possible east-to-west division in the Mediterranean with regard to precipitation (summer and  
334 annual) during the Holocene. They report wet centennial-scale spells in the eastern  
335 Mediterranean during the early Holocene (until 6000 years BP), with dry spells in the western

336 Mediterranean. Mid-Holocene reconstructions show continued wet conditions, with drying  
337 through the late Holocene (Guiot and Kaniewski, 2015). This pattern indicates a see-saw effect  
338 over the last 10,000 years, particularly during dry episodes in the Near and Middle East. Similar  
339 to in our findings, Mauri et al. (2015) also reconstruct high annual precipitation values over  
340 much of the southern Mediterranean, and a weak winter precipitation signal. Mauri et al. (2015)  
341 confirm an east-west dipole for summer precipitation, with conditions drier or close to present  
342 in south-western Europe and wetter in the central and eastern Mediterranean (Fig 2b). These  
343 studies corroborate the hypothesis of an east-to-west division in precipitation during the early  
344 to mid-Holocene in the Mediterranean as proposed by Roberts et al. (2011). Roberts et al.  
345 (2011) suggest the eastern Mediterranean (mainly Turkey and more eastern regions)  
346 experienced higher winter precipitation during the early Holocene, followed by an oscillatory  
347 decline after 6000 yrs BP. Our findings reveal wetter annual and summer conditions in the  
348 eastern Mediterranean, although the winter precipitation signal is less clear. However, the  
349 highest precipitation values reported by Roberts et al. (2011) were from sites located in western-  
350 central Turkey; these sites are absent in the current study. Climate variability in the eastern  
351 Mediterranean during the last 6000 years is also documented in a number of studies based on  
352 multiple proxies (Finné et al., 2011). Most palaeoclimate proxies indicate wet mid-Holocene  
353 conditions (Bar-Matthews et al., 2003; Stevens et al., 2006; Eastwood et al., 2007; Kuhnt et al.,  
354 2008; Verheyden et al., 2008) which agree well with our results; however most of these proxies  
355 are not seasonally resolved.

356 Roberts et al. (2011) and Guiot and Kaniewski (2015) suggest that changes in precipitation in  
357 the western Mediterranean were smaller in magnitude during the early Holocene, while the  
358 largest increases occurred during the mid-Holocene, around 6000-3000 cal BP, before declining  
359 to modern values. Speleothems from southern Iberia suggest a humid early Holocene (9000-  
360 7300 cal BP) in southern Iberia, with equitable rainfall throughout the year (Walczak et al.,  
361 2015) whereas our reconstructions for the Alboran Sea clearly show an amplified precipitation  
362 seasonality (with higher annual/winter and similar to modern summer rainfall) for the Alboran  
363 sites. It is likely that seasonal patterns defining the Mediterranean climate must have been even  
364 stronger in the early Holocene to support the wider development of sclerophyll forests than  
365 present in south Spain (Fletcher et al., 2013).

366 Late Holocene (4000 to 2000 cal yrs BP)

367 Annual precipitation reconstructions suggest drier or near-modern conditions in central Italy,  
368 Adriatic Sea, Siculo-Tunisian strait and Malta (Figs. 2b and 3). In contrast, the Alboran and

369 Aegean Seas remain wetter. Winter and summer precipitation produce opposing patterns; a  
370 clear east-west division still exists for summer precipitation, with a maximum in the eastern  
371 and a minimum over the western and central Mediterranean (Fig. 2b). Winter precipitation  
372 shows the opposite trend, with a minimum in the central Mediterranean (Sicily, Siculo-Tunisian  
373 strait and Malta) and eastern Mediterranean, and a maximum in the western Mediterranean  
374 (Figs. 2b and 3). Our results are also in agreement with lakes and speleothem isotope records  
375 over the Mediterranean for the late Holocene (Roberts et al., 2011), and the Finné et al. (2011)  
376 palaeoclimate synthesis for the eastern Mediterranean. There is a good overall correspondence  
377 between trends and patterns in our reconstruction and that of Mauri et al. (2015), except for the  
378 Alboran Sea. High-resolution speleothem data from southern Iberia show Mediterranean  
379 climate conditions in southern Iberia between 4800 and 3000 cal BP (Walczak et al., 2015)  
380 which is in agreement with our reconstruction. The Mediterranean climate conditions  
381 reconstructed here for the Alboran Sea during the late Holocene is consistent with a climate  
382 reconstruction available from the Middle Atlas (Morocco), which show a trend over the last  
383 6000 years towards arid conditions as well as higher precipitation seasonality between 4000  
384 and 2000 cal yrs BP (Nourelbait et al., 2016). There is also good evidence from many records  
385 to support late Holocene aridification in southern Iberia. Paleoclimatic studies document a  
386 progressive aridification trend since ~7000 cal yr BP (e.g. Carrion et al., 2010; Jimenez-Moreno  
387 et al., 2015; Ramos-Roman et al., 2016), although a reconstruction of the annual precipitation  
388 inferred from pollen data with the Probability Density Function method indicate stable and dry  
389 conditions in the south of the Iberian Peninsula between 9000 and 3000 cal BP (Tarroso et al.,  
390 2016).

391 The current study shows that a prominent feature of late Holocene climate is the east-west  
392 division in summer precipitation: summers were overall dry or near-modern in the central and  
393 western Mediterranean and clearly wetter in the eastern Mediterranean. In contrast, winters  
394 were drier or near-modern in the central and eastern Mediterranean (Fig. 3) while they were  
395 wetter only in the Alboran Sea.

396

### 397 *Data-model comparison*

398 Figure 3 shows the data-model comparisons for the early to mid-Holocene (a) and late Holocene  
399 (b) compared to the Present day control run (in anomalies, with statistical significance hatched.  
400 Encouragingly, there is a good overall correspondence between patterns and trends in pollen-

401 inferred precipitation and model outputs. Caution is required when interpreting climate model  
402 results, however, as many of the changes depicted in Fig. 3 are very small and of marginal  
403 statistical significance, suggesting a high degree of uncertainty around their robustness.

404 For the early to mid-Holocene, both model and data indicate wet annual and summer conditions  
405 in Greece and in the eastern Mediterranean, and drier than today conditions in north Italy. There  
406 are indications of an east to west division in summer precipitation simulated by the climate  
407 model (e.g., between the ocean to the south of Italy and over Greece/Turkey), although the  
408 changes are extremely small with a level of significance of 70% (p-value=0.7). Furthermore, in  
409 the Aegean Sea, the model shows a good match with pollen-based reconstructions, suggesting  
410 that the increased spatial resolution of the regional climate model may help to simulate the  
411 localized, “patchy”, impacts of Holocene climate change, when compared to coarser global  
412 GCMs (Fig. 3). In Italy, the model shows a good match with pollen-based reconstructions with  
413 regards to the contrasting north-south precipitation regimes, but there is little agreement  
414 between model output and climate reconstruction with regard to winter and annual precipitation  
415 in southern Italy. The climate model suggests wetter winter and annual conditions in the far  
416 western Mediterranean (i.e. France, western Iberia and the NW coast of Africa) – similar to  
417 pollen-based reconstructions – and near-modern summer conditions during summers (except in  
418 France and northern Africa). A prominent feature of winter precipitation simulated by the model  
419 and partly supported by the pollen estimates is the reduced early Holocene precipitation  
420 everywhere in the Mediterranean basin except in the south east.

421 Model and pollen-based reconstructions for the late Holocene indicate declining winter  
422 precipitation in the eastern Mediterranean and southern Italy (Sicily and Malta) relative to the  
423 early Holocene. In contrast, late Holocene summer precipitation is higher than today in Greece  
424 and in the eastern Mediterranean and near-modern in the central and western Mediterranean,  
425 and relatively lower than today in south Spain and north Africa. The east-west division in  
426 summer precipitation is strongest during the late Holocene in the proxy data and there are  
427 suggestions that it appears to be consistently simulated in the climate model; the signal is  
428 reasonably clear in the eastern Mediterranean (Greece and Turkey) but non-significant in  
429 central and western Mediterranean (Fig. 3).

430 Our findings can be compared with previous data-model comparisons based on the same set of  
431 climate model experiments; although here we take our reference period as ‘present-day’ (1960-  
432 1990) rather than preindustrial and thus include an additional ‘signal’ from recent  
433 anthropogenic greenhouse gas emissions. Previous comparisons nevertheless suggested that the

434 winter precipitation signal was strongest in the northeastern Mediterranean (near Turkey)  
435 during the early Holocene and that there was a drying trend in the Mediterranean from the early  
436 Holocene to the late Holocene, particularly in the east (Brayshaw et al., 2011a; Roberts et al.,  
437 2011). This is coupled with a gradually weakening seasonal cycle of surface air temperatures  
438 towards the present.

439 It is clear that most global climate models (PMIP2, PMIP3) simulate only very small changes  
440 in summer precipitation in the Mediterranean during the Holocene (Braconnot et al., 2007a,b,  
441 2012; Mauri et al., 2014). The lack of a summer precipitation signal is consistent with the failure  
442 of the northeastern extension of the West African monsoon to reach the southeastern  
443 Mediterranean, even in the early to-mid-Holocene (Brayshaw et al., 2011a). The regional  
444 climate model simulates a small change in precipitation compared to the proxy results, and it  
445 can be robustly identified as statistically significant. This is to some extent unsurprising, insofar  
446 as the regional climate simulations presented here are themselves “driven” by data derived from  
447 a coarse global model (which, like its PMIP2/3 peers, does not simulate an extension of the  
448 African monsoon into the Mediterranean during this time period). Therefore, questions remain  
449 about summer precipitation in the eastern Mediterranean during the Holocene. The underlying  
450 climate dynamics therefore need to be better understood in order to confidently reconcile proxy  
451 data (which suggest increased summer precipitation during the early Holocene in the Eastern  
452 Mediterranean) with climate model results (Mauri et al., 2014). Based on the high-resolution  
453 coupled climate model EC-Earth, Bosmans et al. (2015) show how the seasonality of  
454 Mediterranean precipitation should vary from minimum to maximum precession, indicating a  
455 reduction in precipitation seasonality, due to changes in storm tracks and local cyclogenesis  
456 (i.e. no direct monsoon required). Such high-resolution climate modeling studies (both global  
457 and regional) may prove a key ingredient in simulating the relevant atmospheric processes (both  
458 local and remote) and providing fine-grain spatial detail necessary to compare results to palaeo-  
459 proxy observations.

460 Another explanation proposed by Mauri et al. (2014) is linked to the changes in atmospheric  
461 circulation. Our reconstructed climate characterized by dry winters and wet summers shows a  
462 spatial pattern that is somewhat consistent with modern day variability in atmospheric  
463 circulation rather than simple direct radiative forcing by insolation. In particular, the gross NW-  
464 SE dipole of reconstructed winter precipitation anomalies is perhaps similar to that associated  
465 with a modern-day positive AO/NAO. The west coast of Spain is, however, also wetter in our  
466 early Holocene simulations which would seem to somewhat confound this simple picture of a

467 shift to an NAO+ like state compared to present. In summer, an anti-cyclonic blocking close to  
468 Scandinavia may have caused a more meridional circulation, which brought dry conditions to  
469 northern Europe, but relatively cooler and somewhat wetter conditions to many parts of  
470 southern Europe. It is of note that some climate models which have been used for studying  
471 palaeoclimate have difficulty reproducing this aspect of modern climate (Mauri et al., 2014).  
472 Future work based on transient Holocene model simulations are important, nevertheless,  
473 transient-model simulations have also shown mid-Holocene data-model discrepancies (Fischer  
474 and Jungclaus, 2011; Renssen et al., 2012). It is, however, suggested that further work is  
475 required to fully understand changes in winter and summer circulation patterns over the  
476 Mediterranean (Bosmans et al., 2015).

477

#### 478 *Data limitations*

479 Classic ecological works for the Mediterranean (e.g. Ozenda 1975) highlight how precipitation  
480 limits vegetation type in plains and lowland areas, but temperature gradients take primary  
481 importance in mountain systems. Also, temperature and precipitation changes are not  
482 independent, but interact through bioclimatic moisture availability and growing season length  
483 (Prentice et al., 1996). This may be one reason why certain sites may diverge from model  
484 outputs; the Alboran sites, for example, integrate pollen from the coastal plains through to  
485 mountain (+1500m) elevations. At high elevations within the source area, temperature effects  
486 become be more important than precipitation in determining the forest cover type. Therefore, it  
487 is not possible to fully isolate precipitation signals from temperature changes. Particularly for  
488 the semiarid areas of the Mediterranean, the reconstruction approach probably cannot  
489 distinguish between a reduction in precipitation and an increase in temperature and PET, or vice  
490 versa.

491 Along similar lines, while the concept of reconstructing winter and summer precipitation  
492 separately is very attractive, it may be worth commenting on some limitations. Although  
493 different levels of the severity or length of summer drought are an important ecological  
494 limitation for vegetation, reconstructing absolute summer precipitation can be difficult because  
495 the severity/length of bioclimatic drought is determined by both temperature and precipitation.  
496 We are dealing with a season that has, by definition, small amounts of precipitation that drop  
497 below the requirements for vegetation growth. Elevation is also of concern, as lowland systems  
498 tend to be recharged by winter rainfall, but high mountain systems may receive a significant

499 part of precipitation as snowfall, which is not directly available to plant life. This may be  
500 important in the long run for improving the interpretation of long-term Holocene changes and  
501 contrasts between different proxies, such as lake-levels and speleothems. Although these issues  
502 may initially appear to be of marginal importance, they may nevertheless have a real influence  
503 leading to problems and mismatches between different proxies (e.g. Davis et al., 2003; Mauri  
504 et al., 2015).

505 Another important point is the question of human impact on the Mediterranean vegetation  
506 during the Holocene. Since human activity has influenced natural vegetation, distinguishing  
507 between vegetation change induced by humans and climatic change in the Mediterranean is a  
508 challenge requiring independent proxies and approaches. Therefore links and processes behind  
509 societal change and climate change in the Mediterranean region are increasingly being  
510 investigated (e.g. Holmgren et al., 2016; Gogou et al., 2016; Sadori et al., 2016a). Here, the  
511 behavior of the reconstructed climatic variables between 4000 and 2000 cal yrs BP is likely  
512 to be influenced by non-natural ecosystem changes due to human activities such as the forest  
513 degradation that began in lowlands, progressing to mountainous areas (Carrión et al., 2010).  
514 These human impacts add confounding effects for fossil pollen records and may lead to slightly  
515 biased temperature reconstructions during the late Holocene, likely biased towards warmer  
516 temperatures and lower precipitation. However, if human activities become more marked at  
517 3000 cal yrs BP, they increase significantly over the last millennia (Sadori et al., 2016) which  
518 is not within the time scale studied here. Moreover there is strong agreement between summer  
519 precipitation and independently reconstructed lake-level curves (Magny et al., 2013). For the  
520 marine pollen cores, human influence is much more difficult to interpret given that the source  
521 area is so large, and that, in general, anthropic taxa are not found in marine pollen assemblages.

522

## 523 **Conclusions**

524 The Mediterranean is particularly sensitive to climate change but the extent of future change  
525 relative to changes during the Holocene remains uncertain. Here, we present a reconstruction  
526 of Holocene precipitation in the Mediterranean using an approach based on both terrestrial and  
527 marine pollen records, along with a model-data comparison based on a high resolution regional  
528 model. We investigate climatic trends across the Mediterranean during the Holocene to test the  
529 hypothesis of an alternating north-south precipitation regime, and/or an east-west precipitation  
530 dipole. We give particular emphasis to the reconstruction of seasonal precipitation considering  
531 the important role it plays in this system.

532 Climatic trends reconstructed in this study seem to corroborate the north-south division of  
533 precipitation regimes during the Holocene, with wet conditions in the south-central and eastern  
534 Mediterranean, and dry conditions above 45°N during the early Holocene, while the opposite  
535 pattern dominates during the late Holocene. This study also shows that a prominent feature of  
536 Holocene climate in the Mediterranean is the east-to-west division in precipitation, strongly  
537 linked to the seasonal parameter reconstructed. During the early Holocene, we observe an east-  
538 to-west division with high summer precipitation in Greece and the eastern Mediterranean and  
539 a minimum over the Italy and the western Mediterranean. There was a drying trend in the  
540 Mediterranean from the early Holocene to the late Holocene, particularly in central and eastern  
541 regions but summers in the east remained wetter than today. In contrast, the signal for winter  
542 precipitation is less spatially consistent during the early Holocene, but it clearly shows similar  
543 to present day or drier conditions everywhere in the Mediterranean except in the western basin  
544 during the late Holocene.

545 The regional climate model outputs show a remarkable qualitative agreement with our pollen-  
546 based reconstructions, although it must be emphasised that the changes simulated are typically  
547 very small or of questionable statistical significance. Nevertheless, there are indications that the  
548 east to west division in summer precipitation reconstructed from the pollen records do appear  
549 to be simulated by the climate model. The model results also suggest that parts of the eastern  
550 Mediterranean experienced similar to present day or drier conditions in winter during the early  
551 and late Holocene and wetter conditions in annual and summer during the early and late  
552 Holocene (both consistent with the paleo-records).

553 Although this study has used regional climate model data, it must always be recalled that the  
554 regional model's high-resolution output is strongly constrained by a coarser-resolution global  
555 climate model, and the ability of global models to correctly reproduce large-scale patterns of  
556 change in the Mediterranean over the Holocene remains unclear (e.g. Mauri et al 2015). The  
557 generally positive comparison between model and data presented here may therefore simply be  
558 fortuitous and not necessarily replicated if the output from other global climate model  
559 simulations was downscaled in a similar way. However, it is noted that the use of higher-  
560 resolution regional climate models can offer significant advantages for data-model comparison  
561 insofar as they assist in resolving the inherently "patchy" nature of climate signals and palaeo-  
562 records. Notwithstanding the difficulties of correctly modeling large-scale climate change over  
563 the Holocene (with GCMs), we believe that regional downscaling may still be valuable in

564 facilitating model-data comparison in regions/locations known to be strongly influenced by  
565 local effects (e.g., complex topography).

566

567 **Acknowledgements**

568 This study is a part of the LAMA ANR Project (MSHE Ledoux, USR 3124, CNRS) financially  
569 supported by the French CNRS (National Centre for Scientific Research). Simon Goring is  
570 currently supported by NSF Macrosystems grant 144-PRJ45LP. This is an ISEM contribution  
571 n°XXXX.

572

573 **Figure captions**

574 Figure 1: Locations of terrestrial and marine pollen records along a longitudinal gradient from  
575 west to east and along a latitudinal gradient from northern Italy to Malta. Ombrothermic  
576 diagrams are shown for each site, calculated with the NewLoclim software program and  
577 database, which provides estimates of average climatic conditions at locations for which  
578 no observations are available (ex.: marine pollen cores).

579 Figure 2: Pollen-inferred climate estimates as performed with the Modern Analogues  
580 Technique (MAT): annual precipitation, winter precipitation (winter = sum of  
581 December, January and February precipitation) and summer precipitation (summer =  
582 sum of June, July and August precipitation). Changes in climate are expressed as  
583 differences with respect to the modern values (anomalies, mm/day). The modern values  
584 are derived from the ombrothermic diagrams (cf Fig. 1). Two key intervals of the  
585 Holocene corresponding to the two time slice experiments (Fig. 3) have been chosen:  
586 8000–6000 cal yrs BP (a) and 4000–2000 (b) cal yrs BP. The climate values available  
587 during these periods have been averaged (stars).

588 Figure 3: Data-model comparison for mid and late Holocene precipitation, expressed in  
589 anomaly compared to present-day (mm/day). Simulations are based on a regional model  
590 (Brayshaw et al., 2010): standard model HadAM3 coupled to HadSM3 (dynamical  
591 model) and HadRM3 (high-resolution regional model. The hatching representing  
592 statistical significance refers to the anomalies shown on the same plot – i.e., the  
593 difference between the experiment (either 8000–6000 or 4000–2000) and the Present  
594 day control run. The hatched areas indicate areas where the changes are not significant  
595 (70% rank-significance test). Pollen-inferred climate estimates (stars) are the same as in  
596 Fig. 2: annual precipitation, winter precipitation (winter = sum of December, January  
597 and February precipitation) and summer precipitation (summer = sum of June, July and  
598 August precipitation).

599 Figure 4: Model simulation showing Present day minus Preindustrial precipitation anomalies  
600 (hatching at 70%/statistical significance over the insignificant regions)

601 Table 1: Metadata for the terrestrial and marine pollen records evaluated.

602

603 **References**

- 604 Alpert, P., Baldi, M., Ilani, R., Krichak, S., Price, C., Rodó, X., Saaroni, H., Ziv, B., Kishcha,  
605 P., Barkan, J., Mariotti, A. and Xoplaki, E.: Relations between climate variability in the  
606 Mediterranean region and the Tropics: ENSO, South Asian and African monsoons, hurricanes  
607 and Saharan dust In: Lionello P, Malanotte-Rizzoli P, Boscolo R (eds) Mediterranean  
608 Climate Variability, Amsterdam, Elsevier 149-177, 2006.
- 609 Bar-Matthews, M., Ayalon, A., Gilmour, M., Matthews, A. and Hawkesworth, C.J.: Sea-land  
610 oxygen isotopic relationships from planktonic foraminifera and speleothems in the Eastern  
611 Mediterranean region and their implication for paleorainfall during interglacial intervals,  
612 *Geochimica et Cosmochimica Acta* 67, 3181-3199, 2003.
- 613 Bar-Matthews, M. and Ayalon, A.: Mid-Holocene climate variations revealed by high-  
614 resolution speleothem records from Soreq Cave, Israel and their correlations with cultural  
615 changes, *Holocene*, 21, 163–172, 2011.
- 616 Bartlein, P.J., Harrison, S.P., Brewer, S., Connor, S., Davis, B.A.S., Gajewski, K., Guiot, J.,  
617 Harrison-Prentice, T.I., Henderson, A., Peyron, O., Prentice, I.C., Scholze, M., Seppä, H.,  
618 Shuman, B., Sugita, S., Thompson, R.S., Vial, A.E, Williams, J., and Wu H.: Pollen-based  
619 continental climate reconstructions at 6 and 21 ka: a global synthesis, *Climate Dynamics* 37,  
620 775-802, 2011.
- 621 Bosmans, J.H.C., Drijfhout, S.S., Tuenter, E., Hilgen, F.J., Lourens, L.J. and Rohling, E.J.:  
622 Precession and obliquity forcing of the freshwater budget over the Mediterranean, *Quaternary*  
623 *Science Reviews*, 123, 16-30, 2015.
- 624 Braconnot, P., Otto-Bliesner, B., Harrison, S., Joussaume, S., Peterchmitt, J.-Y., Abe-Ouchi,  
625 A., Crucifix, M., Driesschaert, E., Fichet, Th., Hewitt, C. D., Kageyama, M., Kitoh, A., Lâiné,  
626 A., Loutre, M.-F., Marti, O., Merkel, U., Ramstein, G., Valdes, P., Weber, S. L., Yu, Y., and  
627 Zhao, Y.: Results of PMIP2 coupled simulations of the Mid-Holocene and Last Glacial  
628 Maximum –Part 1: experiments and large-scale features, *Clim. Past*, 3, 261–277, 2007a.
- 629 Braconnot, P., Otto-Bliesner, B., Harrison, S., Joussaume, S., Peterchmitt, J.-Y., Abe-Ouchi,  
630 A., Crucifix, M., Driesschaert, E., Fichet, Th., Hewitt, C. D., Kageyama, M., Kitoh, A.,  
631 Loutre, M.-F., Marti, O., Merkel, U., Ramstein, G., Valdes, P., Weber, L., Yu, Y., and Zhao,  
632 Y.: Results of PMIP2 coupled simula-tions of the Mid-Holocene and Last Glacial Maximum –  
633 Part 2: feedbacks with emphasis on the location of the ITCZ and mid- and high latitudes heat  
634 budget, *Clim. Past*, 3, 279–296, 2007b.

635 Braconnot, P., Harrison, S., Kageyama, M., Bartlein, J., Masson, V., Abe-Ouchi, A., Otto-  
636 Bliesner, B., and Zhao, Y.: Evaluation of climate models using palaeoclimatic data, *Nat. Clim.*  
637 *Change*, 2, 417-424, 2012.

638 Brayshaw, D.J., Hoskins, B. and Black, E.: Some physical drivers of changes in the winter  
639 storm tracks over the North Atlantic and Mediterranean during the Holocene. *Philosophical*  
640 *Transactions of the Royal Society A: Mathematical, Physical and Engineering Sciences*, 368,  
641 5185-5223, 2010.

642 Brayshaw, D.J., Rambeau, C.M.C., and Smith, S.J.: Changes in the Mediterranean climate  
643 during the Holocene: insights from global and regional climate modelling, *Holocene* 21, 15-31,  
644 2011a.

645 Brayshaw, D.J., Black, E., Hoskins, B. and Slingo, J.: Past climates of the Middle East, In:  
646 Mithen, S. and Black, E. (eds.) *Water, Life and Civilisation: Climate, Environment and Society*  
647 *in the Jordan Valley*. International Hydrology Series. Cambridge University Press, Cambridge,  
648 pp. 25-50, 2011b

649 Carrión, J.S., Fernández, S., Jiménez-Moreno, G., Fauquette, S., Gil-Romera, G., González-  
650 Sampériz, P. and Finlayson, C.: The historical origins of aridity and vegetation degradation in  
651 southeastern Spain, *Journal of Arid Environments*, 74, 731-736, 2010.

652 Cheddadi, R., Yu, G., Guiot, J., Harrison, S.P., and Prentice, I.C.: The climate of Europe 6000  
653 years ago, *Climate Dynamics* 13, 1-9, 1997.

654 Colmenero-Hidalgo, E., Flores, J.-A., and Sierro, F.J. Biometry of *Emiliana huxleyi* and its  
655 biostratigraphic significance in the eastern north Atlantic Ocean and Western Mediterranean  
656 Sea in the last 20,000 years, *Marine Micropaleontology*, 46, 247-263, 2002.

657 Colombaroli, D., Vannièrè, B., Chapron, E., Magny, M., and Tinner, W. Fire–vegetation  
658 interactions during the Mesolithic–Neolithic transition at Lago dell’Accesa, Tuscany, Italy, *The*  
659 *Holocene*, 18, 679–692, 2008.

660 Combourieu-Nebout, N., Paterne, M., Turon, J.-L., and Siani, G.: A high-resolution record of  
661 the Last Deglaciation in the Central Mediterranean Sea: palaeovegetation and  
662 palaeohydrological evolution, *Quaternary Sci. Rev.*, 17, 303–332, 1998.

663 Combourieu-Nebout, N., Londeix, L., Baudin, F., and Turon, J.L.: Quaternary marine and  
664 continental palaeoenvironments in the Western Mediterranean Sea (Leg 161, Site 976, Alboran

665 Sea): Palynological evidences, Proceeding of the Ocean Drilling Project, scientific results, 161,  
666 457-468, 1999.

667 Combourieu-Nebout, N., Turon, J.L., Zahn, R., Capotondi, L., Londeix, L., and Pahnke, K.:  
668 Enhanced aridity and atmospheric high pressure stability over the western Mediterranean  
669 during North Atlantic cold events of the past 50 000 years, *Geology*, 30, 863-866, 2002.

670 Combourieu-Nebout, N., Peyron, O., Dormoy, I., Desprat, S., Beaudouin, C., Kotthoff, U., and  
671 Marret, F.: Rapid climatic variability in the west Mediterranean during the last 25 000 years  
672 from high resolution pollen data, *Clim. Past*, 5, 503-521, 2009.

673 Combourieu-Nebout, N., Peyron, O., Bout-Roumazeilles, V., Goring, S., Dormoy, I., Joannin,  
674 S., Sadori, L., Siani, G., and Magny, M.: Holocene vegetation and climate changes in  
675 central Mediterranean inferred from a high-resolution marine pollen record (Adriatic Sea),  
676 *Clim. Past* 9, 2023-2042, 2013.

677 Davis, B. A. S., Brewer, S., Stevenson, A. C., and Guiot, J.: The temperature of Europe during  
678 the Holocene reconstructed from pollen data, *Quaternary Sci. Rev.*, 22, 1701–1716, 2003.

679 Davis, B. A. S. and Brewer, S.: Orbital forcing and role of the latitudinal insolation/ temperature  
680 gradient, *Clim. Dynam.*, 32, 143-165, 2009.

681 De Santis V. and Caldara M. The 5.5–4.5 kyr climatic transition as recorded by the  
682 sedimentation pattern of coastal deposits of the Apulia region, southern Italy, *Holocene*, 2015

683 Desprat, S., Combourieu-Nebout, N., Essallami, L., Sicre, M. A., Dormoy, I., Peyron, O.,  
684 Siani, G., Bout Roumazeilles, V., and Turon, J. L.: Deglacial and Holocene vegetation  
685 and climatic changes in the southern Central Mediterranean from a direct land-sea  
686 correlation, *Clim. Past*, 9, 767–787, 2013.

687 Djamali, M., Gambin, B., Marriner, N., Andrieu-Ponel, V., Gambin, T., Gandouin, E., Médail,  
688 F., Pavon, D., Ponel, P., and Morhange, C.: Vegetation dynamics during the early to mid-  
689 Holocene transition in NW Malta, human impact versus climatic forcing, *Vegetation History*  
690 *and Archaeobotany* 22, 367-380, 2013.

691 Dormoy, I., Peyron, O., Combourieu Nebout, N., Goring, S., Kotthoff, U., Magny, M, and  
692 Pross, J.: Terrestrial climate variability and seasonality changes in the Mediterranean region  
693 between 15,000 and 4,000 years B.P. deduced from marine pollen records, *Clim. Past*, 5, 615-  
694 632, 2009.

695 Drescher-Schneider, R., de Beaulieu, J.L., Magny, M., Walter-Simonnet, A.V., Bossuet, G.,  
696 Millet, L. Brugiapaglia, E., and Drescher A.: Vegetation history, climate and human impact  
697 over the last 15 000 years at Lago dell'Accesa, *Veg. Hist. Archaeobot.*, 16, 279–299, 2007.

698 Eastwood, W.J., Leng, M., Roberts, N. and Davis B.: Holocene climate change in the eastern  
699 Mediterranean region: a comparison of stable isotope and pollen data from Lake Gölhisar,  
700 southwest Turkey, *J. Quaternary Science* 22, 327–341, 2007.

701 Finné, M., Holmgren, K., Sundqvist, H.S., Weiberg, E., and Lindblom, M.: Climate in the  
702 eastern Mediterranean, and adjacent regions, during the past 6000 years, *J. Archaeol. Sci.*, 38,  
703 3153-3173, 2011.

704 Fischer N., and Jungclaus, J. H.: Evolution of the seasonal temperature cycle in a transient  
705 Holocene simulation: orbital forcing and sea-ice, *Clim. Past*, 7, 1139-1148, 2011.

706 Fletcher, W.J., and Sánchez Goñi, M.F.: Orbital- and sub-orbital-scale climate impacts on  
707 vegetation of the western Mediterranean basin over the last 48,000 yr, *Quat. Res.* 70, 451-464,  
708 2008.

709 Fletcher, W.J., Sanchez Goñi, M.F., Peyron, O., and Dormoy, I.: Abrupt climate changes of the  
710 last deglaciation detected in a western Mediterranean forest record, *Clim. Past* 6, 245-264, 2010.

711 Fletcher, W.J., Debret, M., and Sanchez Goñi, M.F.: Mid-Holocene emergence of a low-  
712 frequency millennial oscillation in western Mediterranean climate: Implications for past  
713 dynamics of the North Atlantic atmospheric westerlies, *The Holocene*, 23, 153-166, 2013.

714 Gambin B., Andrieu-Ponel V., Médail F., Marriner N., Peyron O., Montade V., Gambin T.,  
715 Morhange C., Belkacem D., and Djamali M.: 7300 years of vegetation history and quantitative  
716 climate reconstruction for NW Malta: a Holocene perspective, *Clim. Past* 12, 273-297, 2016

717 Geraga, M., Ioakim, C., Lykousis, V., Tsaila-Monopolis, S., and Mylona, G.: The high-  
718 resolution palaeoclimatic and palaeoceanographic history of the last 24,000 years in the central  
719 Aegean Sea, Greece, *Palaeogeogr. Palaeocl.*, 287, 101–115, 2010.

720 Giorgi, F. and Lionello, P.: Climate change projections for the Mediterranean region, *Global*  
721 *Planet. Change*, 63, 90–104, 2008.

722 Gogou, A., Bouloubassi, I., Lykousis, V., Arnaboldi, M., Gaitani, P., and Meyers, P.A.: Organic  
723 geochemical evidence of abrupt late glacial- Holocene climate changes in the North Aegean  
724 Sea, *Palaeogeogr. Palaeocl.*, 256, 1 – 20, 2007.

725 Gogou, A., Triantaphyllou, M., Xoplaki, E., Izdebski, A., Parinos, C., Dimiza, M., Bouloubassi,  
726 I., Luterbacher, J., Kouli, K., Martrat, B., Toreti, A., Fleitmann, D., Rousakis, G., Kaberi, H.,  
727 Athanasiou, M., and Lykousis, V.: Climate variability and socio-environmental changes in the  
728 northern Aegean (NE Mediterranean) during the last 1500 years, *Quaternary Science Reviews*,  
729 136, 209-228, 2016.

730 Guiot J.: Methodology of the last climatic cycle reconstruction in France from pollen data,  
731 *Palaeogeography, Palaeoclimatology, Palaeoecology*, 80, 49–69, 1990.

732 Guiot, J. and Kaniewski, D.: The Mediterranean Basin and Southern Europe in a warmer world:  
733 what can we learn from the past? *Front. Earth Sci.*, 18, 2015.

734 Hargreaves, J.C., Annan, J.D., Ohgaito, R., Paul, A., and Abe-Ouchi, A.: Skill and reliability  
735 of climate model ensembles at the Last Glacial Maximum and mid-Holocene, *Clim. Past*, 9,  
736 811-823, 2013.

737 Heiri, O., Brooks, S.J., Renssen, H., and 26 authors: Validation of climate model-inferred  
738 regional temperature change for late-glacial Europe, *Nature Communications* 5, 4914, 2014.

739 Heusser, L.E., and Balsam W.L.: Pollen distribution in the N.E. Pacific ocean, *Quaternary*  
740 *Research*, 7, 45-62, 1977.

741 Hewitt, C.D., Senior, C.A., and Mitchell, J.F.B. :The impact of dynamic sea-ice on the  
742 climatology and sensitivity of a GCM: A study of past, present and future climates, *Climate*  
743 *Dynamics* 17: 655–668, 2001.

744 Holmgren, K., Gogou, A., Izdebski, A., Luterbacher, J., Sicre, M.A., and Xoplaki, A.:  
745 Mediterranean Holocene Climate, Environment and Human Societies, *Quaternary Science*  
746 *Reviews*, 136, 1-4, 2016.

747 Ioakim, Chr., Triantaphyllou, M., Tsaila-Monopolis, S., and Lykousis, V.: New  
748 micropalaeontological records of Eastern Mediterranean marine sequences recovered offshore  
749 of Crete, during HERMES cruise and their palaeoclimatic paleoceanographic significance. *Acta*  
750 *Naturalia de “L’Ateneo Parmense”*, 45(1/4): p. 152. In: *Earth System Evolution and the*  
751 *Mediterranean Area from 23 Ma to the Present”*, 2009.

752 Jimenez-Moreno, G., Rodriguez-Ramirez, A., Perez-Asensio, J.N., Carrion, J.S., Lopez-Saez,  
753 J.A, Villarías-Robles J., Celestino-Perez, S., Cerrillo-Cuenca, E., Leon, A., and Contreras, C.:  
754 Impact of late-Holocene aridification trend, climate variability and geodynamic control on the  
755 environment from a coastal area in SW Spain, *Holocene*, 1-11, 2015

756 Joannin, S., Vanni re, B., Galop, D., Peyron, O., Haas, J.N., Gilli, A., Chapron, E., Wirth, S.,  
757 Anselmetti, F., Desmet, M., and Magny, M.: Climate and vegetation changes during the  
758 Lateglacial and Early-Mid Holocene at Lake Ledro (southern Alps, Italy), *Clim. Past* 9, 913-  
759 933, 2013.

760 Joannin, S., Brugiapaglia, E., de Beaulieu, J.L, Bernardo, L., Magny, M., Peyron, O., Goring,  
761 S., and Vanni re, B.: Pollen-based reconstruction of Holocene vegetation and climate in  
762 southern Italy: the case of Lago Trifoglietti., *Clim. Past*, 8, 1973-1996, 2012.

763 Kotthoff, U., Pross, J., M ller, U.C., Peyron, O., Schmiedl, G., and Schulz, H. Climate  
764 dynamics in the borderlands of the Aegean Sea during formation of Sapropel S1 deduced from  
765 a marine pollen record, *Quaternary Sci. Rev.*, 27, 832–845, 2008.

766 Kotthoff, U., Koutsodendris, A., Pross, J., Schmiedl, G., Bornemann, A., Kaul, C., Marino, G.,  
767 Peyron, O., and Schiebel, R. Impact of late glacial cold events on the Northern Aegean region  
768 reconstructed from marine and terrestrial proxy data, *J. Quat. Sci.*, 26, 86-96, 2011.

769 Kouli, K., Gogou, A., Bouloubassi, I., Triantaphyllou, M.V., Ioakim, Chr, Katsouras, G.,  
770 Roussakis, G., and Lykousis, V.: Late postglacial paleoenvironmental change in the  
771 northeastern Mediterranean region: Combined palynological and molecular biomarker  
772 evidence, *Quatern. Int.*, 261, 118-127, 2012.

773 Kuhnt, T., Schmiedl, G., Ehrmann, W., Hamann, Y., and Andersen, N.: Stable isotopic  
774 composition of Holocene benthic foraminifers from the eastern Mediterranean Sea: past  
775 changes in productivity and deep water oxygenation, *Palaeogeography, Palaeoclimatology,*  
776 *Palaeoecology* 268, 106-115, 2008.

777 Lionello, P, Malanotte-Rizzoli, P, Boscolo, R, Alpert, P, Artale, V, Li, L., et al.: The  
778 Mediterranean climate: An overview of the main characteristics and issues. In: Lionello P,  
779 Malanotte-Rizzoli P and Boscolo R (eds) *Mediterranean Climate Variability. Developments in*  
780 *Earth & Environmental Sciences* 4, Elsevier, 1–26, 2006.

781 Lionello, P. (Ed.): *The climate of the Mediterranean region: From the past to the future,*  
782 Elsevier, ISBN: 9780124160422, 2012.

783 Luterbacher, J., Garc a-Herrera, R., Akcer-On, S., Allan R., Alvarez-Castro M.C, and 41  
784 authors: A review of 2000 years of paleoclimatic evidence in the Mediterranean. In: Lionello,  
785 P. (Ed.), *The Climate of the Mediterranean region: From the past to the future,* Elsevier,  
786 Amsterdam, The Netherlands, 2012.

787 Magny, M., de Beaulieu, J.L., Drescher-Schneider, R., Vanni re, B., Walter-Simonnet, A.V.,  
788 Miras, Y., Millet, L., Bossuet, G., Peyron, O., Brugiapaglia, E., and Leroux, A.: Holocene  
789 climate changes in the central Mediterranean as recorded by lake-level fluctuations at Lake  
790 Accessa (Tuscany, Italy), *Quaternary Sci. Rev.* 26, 1736–1758, 2007.

791 Magny, M., Vanni re, B., Zanchetta, G., Fouache, E., Touchais, G., Petrika, L., Coussot, C.,  
792 Walter-Simonnet, A.V., and Arnaud, F.: Possible complexity of the climatic event around 4300-  
793 3800 cal BP in the central and western Mediterranean, *Holocene*, 19, 823-833, 2009.

794 Magny, M., Vanni re, B., Calo, C., Millet, L., Leroux, A., Peyron, O., Zanchetta, G., La Mantia,  
795 T. and Tinner, W.: Holocene hydrological changes in south-western Mediterranean as recorded  
796 by lake-level fluctuations at Lago Preola, a coastal lake in southern Sicily, Italy, *Quaternary*  
797 *Sci. Rev.*, 30, 2459-2475, 2011.

798 Magny, M., Joannin, S., Galop, D., Vanni re, B., Haas, J.N, Bassetti, M., Bellintani, P.,  
799 Scandolari, R., and Desmet, M.: Holocene palaeohydrological changes in the northern  
800 Mediterranean borderlands as reflected by the lake-level record of Lake Ledro, northeastern  
801 Italy, *Quaternary Res.*, 77, 382-396, 2012a.

802 Magny, M., Peyron, O., Sadori, L., Ortu, E., Zanchetta, G., Vanni re, B., and Tinner, W.:  
803 Contrasting patterns of precipitation seasonality during the Holocene in the south- and north-  
804 central Mediterranean, *J. Quaternary Sci.*, 27, 290–296, 2012b.

805 Magny, M. and 29 authors: North-south palaeohydrological contrasts in the central  
806 Mediterranean during the Holocene: tentative synthesis and working hypotheses, *Clim. Past* 9,  
807 2043-2071, 2013.

808 Mauri, A., Davis, B., Collins, P.M. and Kaplan, J.: The climate of Europe during the Holocene:  
809 A gridded pollen-based reconstruction and its multi-proxy evaluation, *Quat. Sc. Rev.* 112, 109-  
810 127, 2014.

811 Mauri, A., Davis, B., Collins, P.M. and Kaplan, J.: The influence of atmospheric circulation on  
812 the mid-Holocene climate of Europe: A data–model comparison, *Clim. Past* 10, 1925-1938,  
813 2015.

814 Morrill, C., Anderson, D.M, Bauer, B.A, Buckner, R.E., Gille, P., Gross, W.S., Hartman, M.,  
815 and Shah, A.: Proxy benchmarks for intercomparison of 8.2 ka simulations, *Clim. Past* 9, 423-  
816 432, 2013.

817 Naughton, F., Sanchez Goñi, M.F., Desprat, S., Turon, J.L., Duprat, J., Malaizé, B., Joli, C.,  
818 Cortijo, E., Drago, T., and Freitas, M.C.: Present-day and past (last 25 000 years) marine pollen  
819 signal off western Iberia, *Marine Micropaleontology* 62, 91-114, 2007.

820 Nourelbait, M., Rhoujjati, A., Benkaddour, A., Carré, M., Eynaud, F., Martinez, P. and  
821 Cheddadi, R.: Climate change and ecosystems dynamics over the last 6000 years in the Middle  
822 Atlas, Morocco, *Clim. Past* 12, 1029-1042, 2016.

823 Peyron, O., Goring, S., Dormoy, I., Kotthoff, U., Pross, J., de Bealieu, J.L., Drescher-  
824 Schneider, R., and Magny, M.: Holocene seasonality changes in the central Mediterranean  
825 region reconstructed from the pollen sequences of Lake Accessa (Italy) and Tenaghi Philippon  
826 (Greece), *Holocene*, 21, 131-146, 2011.

827 Peyron, O., Magny, M., Goring, S., Joannin, S., de Beaulieu, J.-L., Brugiapaglia, E., Sadori, L.,  
828 Garfi, G., Kouli, K., Ioakim, C., and Combourieu-Nebout, N. Contrasting patterns of climatic  
829 changes during the Holocene in the central Mediterranean (Italy) reconstructed from pollen  
830 data, *Clim. Past* 9, 1233-2013, 2013.

831 Pope, V.D., Gallani, M.L., Rowntree, R.R. and Stratton, R.A.: The impact of new physical  
832 parameterizations in the Hadley Centre climate model: HadAM3, *Climate Dynamics*, 16, 123-  
833 146, 2000.

834 Pross, J., Kotthoff, U., Müller, U.C., Peyron, O., Dormoy, I., Schmiedl, G., Kalaitzidis, S., and  
835 Smith, A.M.: Massive perturbation in terrestrial ecosystems of the Eastern Mediterranean  
836 region associated with the 8.2 kyr climatic event, *Geology*, 37, 887-890, 2009.

837 Pross, J., Koutsodendris, A., Christanis, K., Fischer, T., Fletcher, W.J., Hardiman, M.,  
838 Kalaitzidis, S., Knipping, M., Kotthoff, U., Milner, A.M., Müller, U.C., Schmiedl, G., Siavalas,  
839 G., Tzedakis, P.C., and Wulf, S.: The 1.35-Ma-long terrestrial climate archive of Tenaghi  
840 Philippon, northeastern Greece: Evolution, exploration and perspectives for future research,  
841 *Newsletters on Stratigraphy*, 48, 253-276, 2015.

842 Ramos-Román, M.J., Jiménez-Moreno, G., Anderson, R.S., García-Alix, A., Toney, J.L.,  
843 Jiménez-Espejo, F.J. and Carrión, J.S.: Centennial-scale vegetation and North Atlantic  
844 Oscillation changes during the Late Holocene in the southern Iberia, *Quaternary Science*  
845 *Reviews*, 143, 84-98, 2016.

846 Renssen, H., Seppa, H., Crosta, X., Goosse, H., and Roche, D.M.: Global characterization of  
847 the Holocene Thermal Maximum, *Quat. Sci. Rev.*, 48, 7-19, 2012.

848 Roberts, N., Brayshaw, D., Kuzucuoğlu, C., Perez, R., and Sadori, L.: The mid-Holocene  
849 climatic transition in the Mediterranean: Causes and consequences, *Holocene*, 21, 3-13, 2011.

850 Roberts, N., Moreno, A., Valero-Garces, B. L., Corella, J. P., Jones, M., Allcock, S., et al.  
851 Palaeolimnological evidence for an east-west climate see-saw in the mediterranean since AD  
852 900, *Glob. Planet. Change*, 84-85, 23-34, 2012.

853 Rohling, E.J., Cane, T.R., Cooke, S., Sprovieri, M., Bouloubassi, I., Emeis, K.C. et al: African  
854 monsoon variability during the previous interglacial maximum, *Earth Planet. Sc. Lett.*, 202, 61-  
855 75, 2002.

856 Sadori, L. and Narcisi, B.: The postglacial record of environmental history from Lago di  
857 Pergusa, Sicily, *Holocene*, 11, 655-671, 2001.

858 Sadori, L. and Giardini, M.: Charcoal analysis, a method to study vegetation and climate of the  
859 Holocene: The case of Lago di Pergusa, Sicily (Italy), *Geobios-Lyon*, 40, 173-180, 2007.

860 Sadori, L., Zanchetta, G., and Giardini, M.: Last Glacial to Holocene palaeoenvironmental  
861 evolution at Lago di Pergusa (Sicily, Southern Italy) as inferred by pollen, microcharcoal, and  
862 stable isotopes, *Quatern. Int.*, 181, 4-14, 2008.

863 Sadori, L., Jahns, S., and Peyron, O.: Mid-Holocene vegetation history of the central  
864 Mediterranean, *Holocene*, 21, 117-129, 2011.

865 Sadori, L., Ortu, E., Peyron, O., Zanchetta, G., Vannièrè, B., Desmet, M., and Magny, M.: The  
866 last 7 millennia of vegetation and climate changes at Lago di Pergusa (central Sicily, Italy),  
867 *Clim. Past*, 9, 1969-1984, 2013.

868 Sadori, L., Giraudi, C. Masi, A., Magny, M., Ortu, E., Zanchetta, G., and Izdebski, A. Climate,  
869 environment and society in southern Italy during the last 2000 years. A review of the  
870 environmental, historical and archaeological evidence, *Quaternary Science Reviews*, 136, 173-  
871 188, 2016a.

872 Sadori, L., Koutsodendris, A., Masi, A., Bertini, A., Combourieu-Nebout, N., Francke, A.,  
873 Kouli, K., Joannin, S., Mercuri, A.M, Panagiotopoulos, K., Peyron, O., Torri, P., Wagner, B.,  
874 Zanchetta, G., and Donders, T.H.: Pollen-based paleoenvironmental and paleoclimatic change  
875 at Lake Ohrid (SE Europe) during the past 500 ka, *Biogeosciences*, 12, 15461-15493, 2016b.

876 Schemmel, F., Niedermeyer, E.M., Schwab-Lavrič, V., Gleixner, G., Pross, J., and Mulch, A.:  
877 Plant-wax dD values record changing Eastern Mediterranean atmospheric circulation patterns  
878 during the 8.2 ka BP climatic event, *Quaternary Science Reviews*, 133, 96-107, 2016.

879 Stevens, L.R., Ito, E., Schwalb, A., and Wright, H.E.: Timing of atmospheric precipitation in  
880 the Zagros Mountains inferred from a multi-proxy record from Lake Mirabad, Iran, *Quat. Res.*  
881 66, 494-500, 2006.

882 Tarroso, P., Carrión, J., Dorado-Valiño, M., Queiroz, P., Santos, L., Valdeolmillos-Rodríguez,  
883 A., Célio Alves, P., Brito, J. C., and Cheddadi, R.: Spatial climate dynamics in the Iberian  
884 Peninsula since 15 000 yr BP, *Clim. Past*, 12, 1137-1149, 2016.

885 Triantaphyllou, V., Antonarakou, A., Kouli, K., Dimiza, M., Kontakiotis, G., Papanikolaou,  
886 M.D. et al.: Late Glacial–Holocene ecostratigraphy of the south-eastern Aegean Sea, based on  
887 plankton and pollen assemblages, *Geo-Mar. Lett.*, 29, 249-267, 2009a.

888 Triantaphyllou, M.V., Ziveri, P., Gogou, A., Marino, G., Lykousis, V., Bouloubassi, I., Emeis,  
889 K.-C., Kouli, K., Dimiza, M., Rosell-Mele, A., Papanikolaou, M., Katsouras, G., and Nunez,  
890 N.: Late Glacial-Holocene climate variability at the south-eastern margin of the Aegean Sea,  
891 *Mar. Geol.*, 266, 182-197, 2009b.

892 Triantaphyllou, M.V., Gogou, A., Bouloubassi, I., Dimiza, M., Kouli, K., Rousakis, A.G.,  
893 Kotthoff, U., Emeis, K.C., Papanikolaou, M., Athanasiou, M., Parinos, C., Ioakim, C., V. and  
894 Lykousis, V.: Evidence for a warm and humid Mid-Holocene episode in the Aegean and  
895 northern Levantine Seas (Greece, NE Mediterranean), *Regional Environmental Change*, 14,  
896 1697-1712, 2014.

897 Triantaphyllou, M.V., Gogou, A., Dimiza, M.D., Kostopoulou, S., Parinos, C., Roussakis, G.,  
898 Geraga, M., Bouloubassi, I., Fleitmann, D., Zervakis, V., Velaoras, D., Diamantopoulou, A.,  
899 Sampatakis, A. and Lykousis, V.: Holocene Climate Optimum centennial-scale  
900 paleoceanography in the NE Aegean Sea (Mediterranean Sea), *Geo-Marine Letters*, 36, 51-66,  
901 2016.

902 Trigo R.M. and 21 coauthors: Relations between variability in the Mediterranean region and  
903 Mid-latitude variability. In: Lionello P, Malanotte-Rizzoli P., Boscolo R., Eds., *The*  
904 *Mediterranean Climate: An overview of the main characteristics and issues*. Elsevier,  
905 Amsterdam, 2006.

906 Tzedakis, P.C.: Seven ambiguities in the Mediterranean palaeoenvironmental narrative,  
907 *Quaternary Sci. Rev.*, 26, 2042-2066, 2007.

908 Vanni re, B., Power, M.J., Roberts, N., Tinner, W., Carrion, J., Magny, M., Bartlein, P., and  
909 Contributors Data: Circum-Mediterranean fire activity and climate changes during the mid  
910 Holocene environmental transition (8500-2500 cal yr BP), *Holocene*, 21, 53-73, 2011.

911 Vanni re, B., Magny, M., Joannin, S., Simonneau, A., Wirth, S.B., Hamann, Y., Chapron,  
912 E., Gilli, A., Desmet, M., and Anselmetti, F.S.: Orbital changes, variation in solar activity and  
913 increased anthropogenic activities: controls on the Holocene flood frequency in the Lake Ledro  
914 area, Northern Italy, *Clim. Past*, 9, 1193-1209, 2013.

915 Verheyden S., Nader F.H., Cheng H.J., Edwards L.R. and Swennen R.: Paleoclimate  
916 reconstruction in the Levant region from the geochemistry of a Holocene stalagmite from the  
917 Jeita cave, Lebanon, *Quaternary Research*, 70, 368-381, 2008.

918 Walczak, I.W., Baldini, J.U.L., Baldini, L.M., Mcdermott, F., Marsden, S., Standish, C.D,  
919 Richards, D.A., Andreo, B and Slater J.: Reconstructing high-resolution climate using CT  
920 scanning of unsectioned stalagmites: A case study identifying the mid-Holocene onset of the  
921 Mediterranean climate in southern Iberia, *Quaternary Science Reviews* 127, 117-128, 2015.

922 Wilks D. S.: *Statistical methods in the atmospheric sciences* (Academic Press, San Diego, CA),  
923 1995.

924 Wood, S.N. Fast stable restricted maximum likelihood and marginal likelihood estimation of  
925 semiparametric generalized linear models. *J. of the Royal Statistical Society* 73(1), 3-36, 2011.

926 Wu, H., Guiot, J., Brewer, S., and Guo, Z.: Climatic changes in Eurasia and Africa at  
927 the Last Glacial Maximum and mid-Holocene: reconstruction from pollen data using inverse  
928 vegetation modelling, *Clim. Dyn.*, 29, 211-229, 2007.

929 Zanchetta, G., Borghini, A., Fallick, A.E., Bonadonna, F.P., and Leone, G.: Late Quaternary  
930 palaeohydrology of Lake Pergusa (Sicily, southern Italy) as inferred by stable isotopes of  
931 lacustrine carbonates, *J. Paleolimnol.*, 38, 227-239, 2007.

932 Zhorniyak, L.V., Zanchetta, G., Drysdale, R.N., Hellstrom, J.C., Isola, I., Regattieri, E., Piccini,  
933 L., Baneschi, I., and Couchoud, I.: Stratigraphic evidence for a ‘‘pluvial phase’’ between ca.  
934 8200-7100 ka from Renella cave (Central Italy), *Quat. Sci. Rev.*, 30, 409-417, 2011.

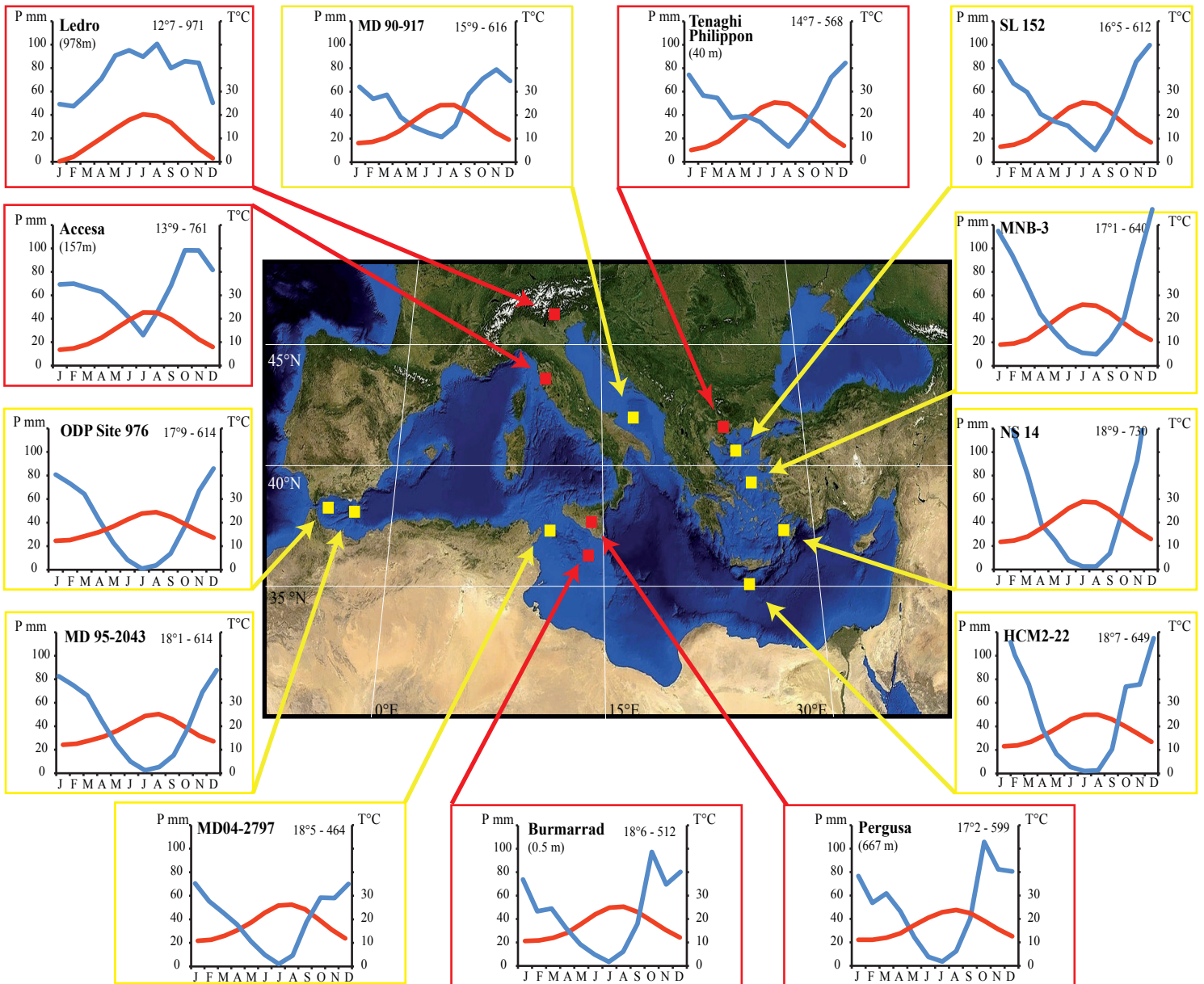
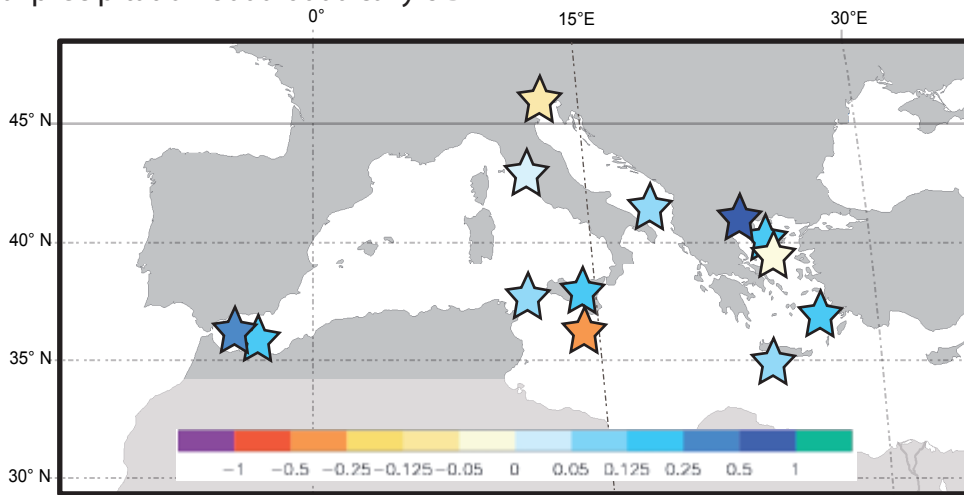


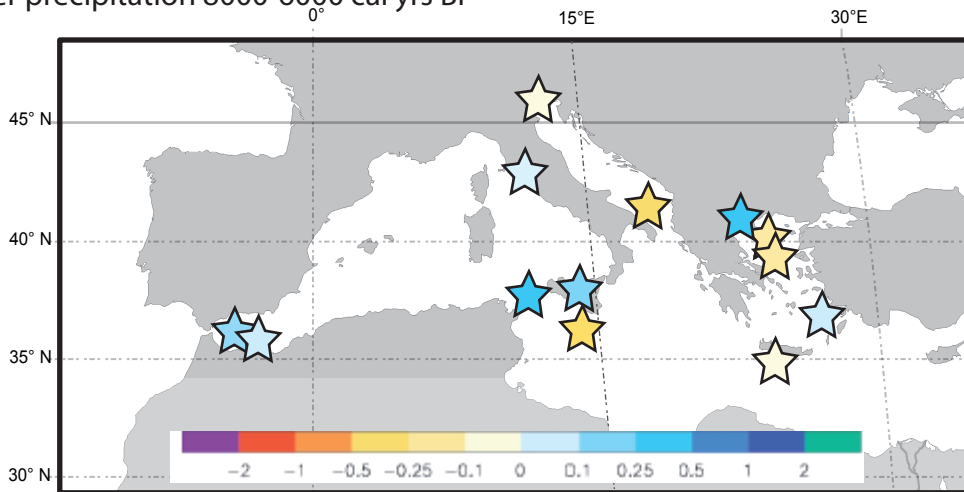
**Figure 1: Locations of terrestrial (red) and marine (yellow) pollen records.**

Ombrothermic diagrams are calculated with the NewLoclim software, which provides estimates of average climatic conditions at locations for which no observations are available (ex.: marine pollen cores).

### Annual precipitation 8000-6000 cal yrs BP



### Winter precipitation 8000-6000 cal yrs BP



### Summer precipitation 8000-6000 cal yrs BP

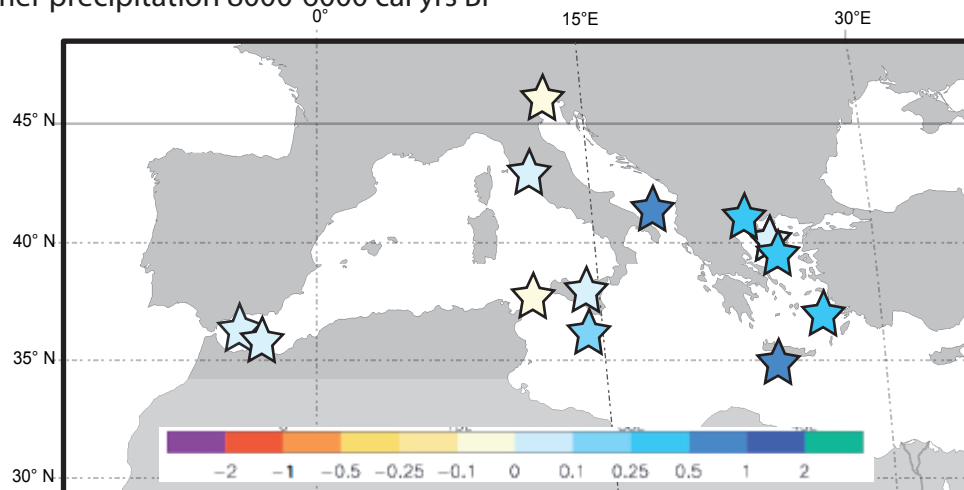
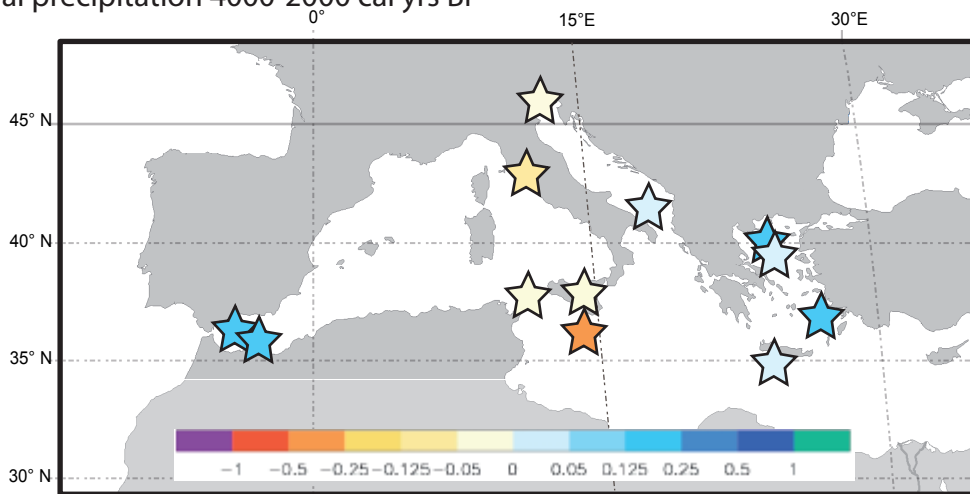


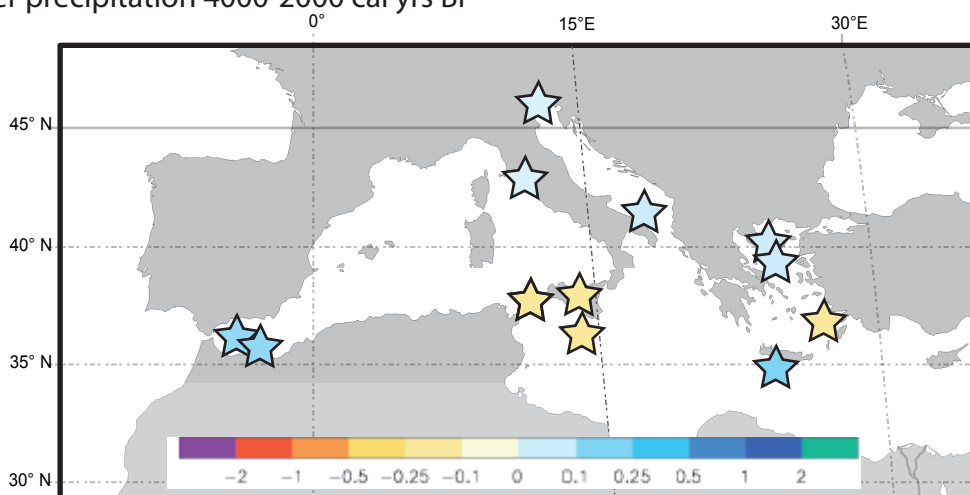
### Figure 2a: 8000-6000 cal years BP

Pollen-inferred climate estimates as performed with the Modern Analogues Technique: annual precipitation, winter precipitation (winter = sum of December, January and February precipitation) and summer precipitation (summer = sum of June, July and August precipitation). Changes in climate are expressed as differences with respect to the modern values (anomalies, mm/day), which are derived from the ombrothermic diagrams (cf Fig. 1). Climate values reconstructed during the 8000-6000 cal yrs BP have been averaged (stars).

### Annual precipitation 4000-2000 cal yrs BP



### Winter precipitation 4000-2000 cal yrs BP



### Summer precipitation 4000-2000 cal yrs BP

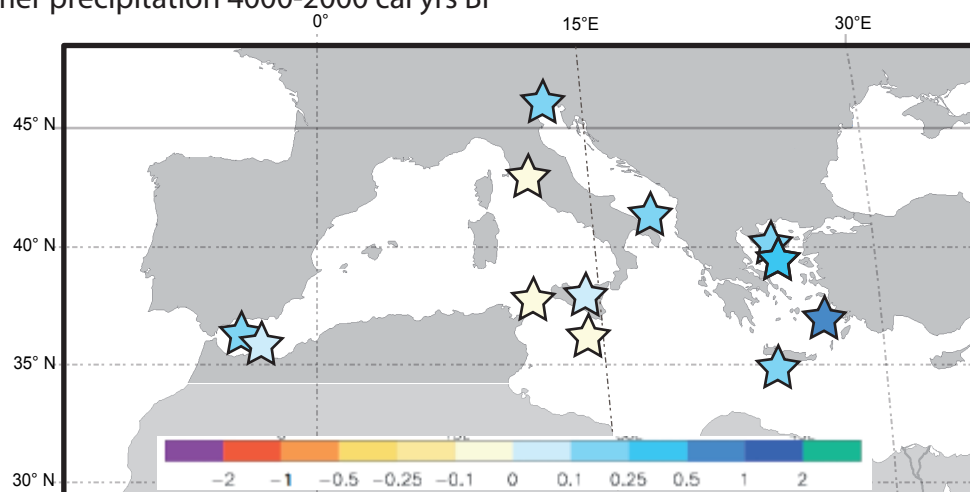
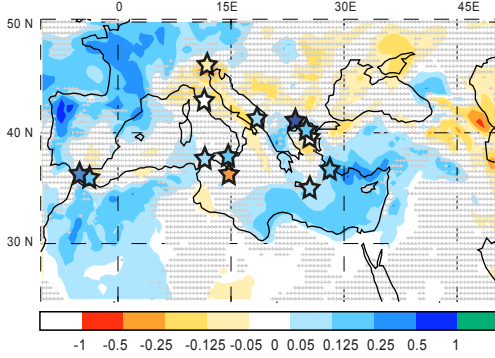


**Figure 2b: 4000-2000 cal yrs BP**

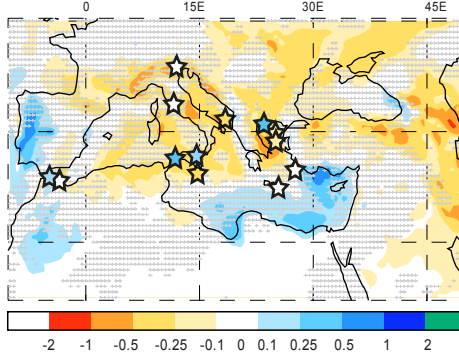
Pollen-inferred climate estimates as performed with the Modern Analogues Technique: annual precipitation, winter precipitation (winter = sum of December, January and February precipitation) and summer precipitation (summer = sum of June, July and August precipitation). Changes in climate are expressed as differences with respect to the modern values (anomalies, mm/day), which are derived from the ombrothermic diagrams (cf Fig. 1). Climate values reconstructed during the 4000-2000 cal yrs BP have been averaged (stars).

### Mid-Holocene: 8000 to 6000 cal BP

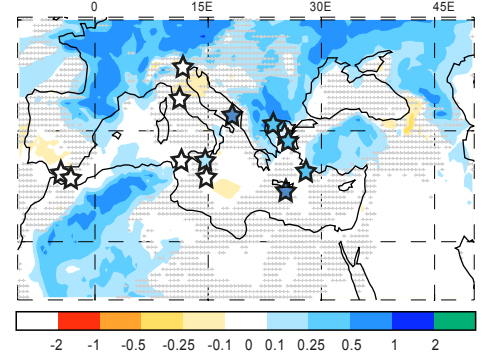
(a) Annual precipitation (anomalie mm/day)



(b) winter precipitation (anomalie mm/day)



(c) summer precipitation (anomalie mm/day)



### Late Holocene: 4000 to 2000 cal BP

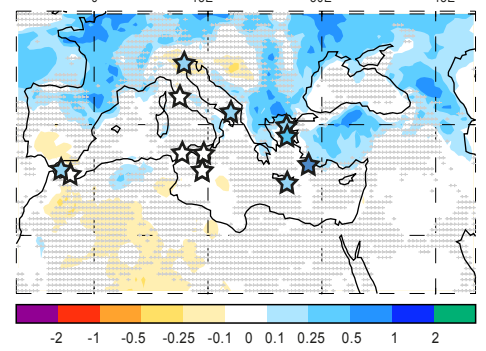
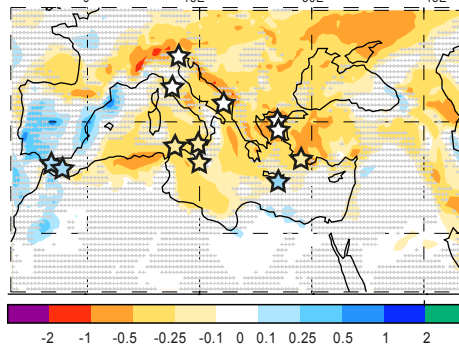
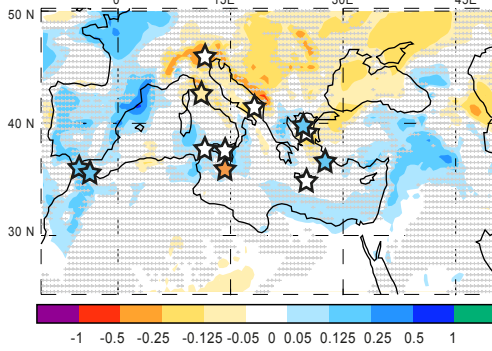


**Figure 3: Data-model comparison for mid and late Holocene precipitation, expressed in anomaly (mm/day)**

Simulations are based on a regional model (Brayshaw et al., 2010): standard model HadAM3 coupled to HadSM3 and HadRM3 (high-resolution regional model). The hatched areas indicate areas where the changes are not significant (threshold used here 70%). Pollen-inferred climate estimates (stars) are the same as in Fig.2: annual precipitation, winter precipitation and summer precipitation .

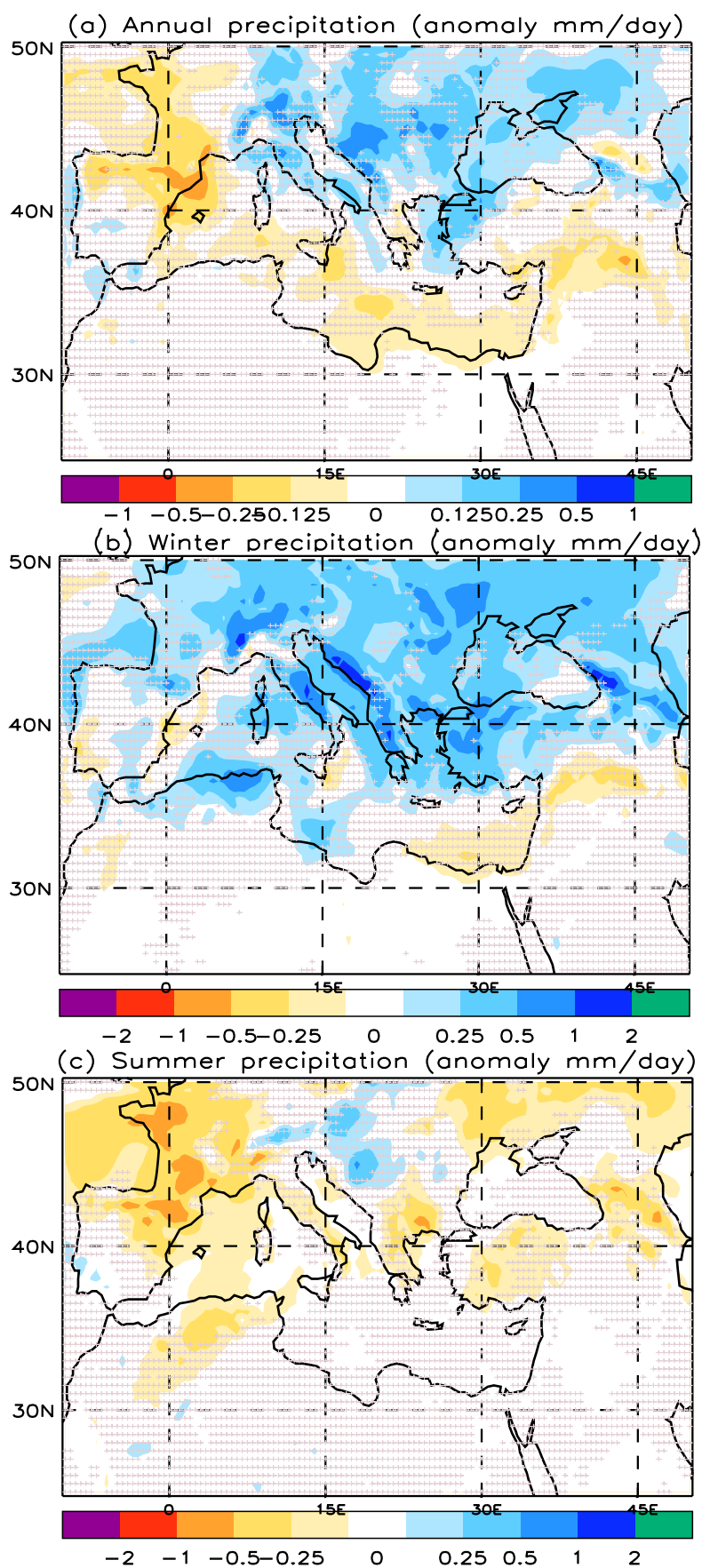


**Figure 4: Model simulation showing Present day minus Preindustrial precipitation anomalies**  
(hatching at 70%/statistical significance over the insignificant regions)

<b>Terrestrial pollen records</b>					
	<b>Longit.</b>	<b>Latitude</b>	<b>Elev. (m a.s.l)</b>	<b>Temporal resolution</b>	<b>References (non- exhaustive)</b>
<b>Ledro</b> (North Italy)	10°76'E	45°87'N	652	8000-6000: 71 4000-2000: 60 10966-10: 66	Joannin et al. (2013), Magny et al. (2009, 2012a), Vanni�re et al. (2013), Peyron et al. (2013)
<b>Accesa</b> (Central Italy)	10°53'E	42°59'N	157	8000-6000: 90 4000-2000 : 133 11029-100: 97	Drescher-Schneider et al. (2007), Magny et al. (2007, 2013), Colombaroli et al. (2008), Sadori et al. (2011), Vanni�re et al. (2011), Peyron et al. (2011, 2013)
<b>Trifoglietti</b> (Southern Italy)	16°01'E	39°33'N	1048	8000-6000: 95 4000-2000: 86 9967-14: 73	Joannin et al. (2012), Peyron et al. (2013)
<b>Pergusa</b> (Sicily)	14°18'E	37°31'N	667	8000-6000: 166 4000-2000: 90 12749-53: 154	Sadori and Narcisi (2001); Sadori et al. (2008, 2011, 2013, 2016b); Magny et al. (2011, 2013)
<b>Tenaghi Philippon</b> (Greece)	24°13.4'E	40°58.4'N	40	8000-6000: 64 4000-2000: no 10369-6371:53	Pross et al. (2009, 2015), Peyron et al. (2011), Schemmel et al., (2016)
<b>Burmarrad</b> (Malta)	14°25'E	35°56'N	0.5	8000-6000: 400 4000-2000: 285 6904-1730: 110	Djamali et al. (2013), Gambin et al., (2016)
<b>Marine pollen records</b>					
	<b>Longit.</b>	<b>Latitude</b>	<b>Water- depth</b>	<b>Temporal resolution</b>	<b>References</b>
<b>ODP 976</b> (Alboran Sea)	4°18'W	36°12' N	1108	8000-6000: 142 4000-2000: 181 10903-132: 129	Combourieu-Nebout et al. (1999, 2002, 2009) ; Dormoy et al., (2009)
<b>MD95-2043</b> (Alboran Sea)	2°37'W	36°9'N	1841	8000-6000: 111 4000-2000: 142 10952-1279: 106	Fletcher and S�nchez Go�i (2008); Fletcher et al., (2010)
<b>MD90-917</b> (Adriatic Sea)	17°37'E	41°97'N	845	8000-6000: 90 4000-2000: 333 10495-2641: 122	Combourieu-Nebout et al. (2013)
<b>MD04-2797</b> (Siculo-Tunisian strait)	11°40'E	36°57'N	771	8000-6000: 111 4000-2000: 666 10985-2215: 127	Desprat et al. (2013)
<b>SL152</b> (North Aegean Sea)	24°36' E	40°19' N	978	8000-6000: 60 4000-2000: 95 9999-0: 76	Kotthoff et al. (2008, 2011), Dormoy et al. (2009).
<b>NS14</b> (South Aegean Sea)	27°02'E	36°38'N	505	8000-6000: 80 4000-2000: 333 9988-2570: 107	Kouli et al. (2012) ; Gogou et al. (2007); Triantaphyllou et al. (2009a, b)
<b>HCM2/22</b> (South Crete)	24°53'E	34°34 N	2211	8000-6000: 181 4000-2000: 333 8091-2390: 247	Ioakim et.al. (2009) ; Kouli et al, (2012) ; Triantaphyllou et al. (2014)

---

<b>MNB-3</b> (North Aegean Sea)	25°00'E	39°15'N	800	8000-6000: 153 4000-2000: 166 8209-2273: 138	Geraga et al. (2010) ; Kouli et al., (2012) ; Triantaphyllou et al, (2014)
---------------------------------	---------	---------	-----	--	--

---

Table 1: Metadata for the terrestrial and marine pollen records evaluated. The temporal resolution is calculated for the two periods (8000-6000 and 4000-2000) and for the entire record.